



Field effect experiments on transition metal oxides

E. Bellingeri

CNR-INFM - LAMIA Corso Perrone 24 16152 Genova Italy

Oxide Electronics Group

Director A.S. Siri*

D. Marré*, I. Pallecchi, L. Pellegrino

G. Canu, A. Caviglia

*Università di Genova Dipartimento di Fisica

Via Dodecaneso 33 16146 Genova

Italy

Superconductivity & technological transfer

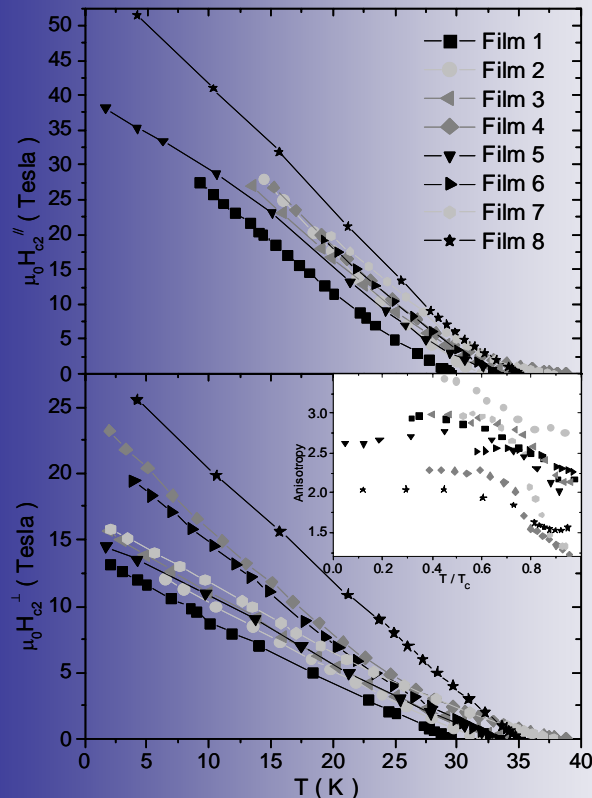
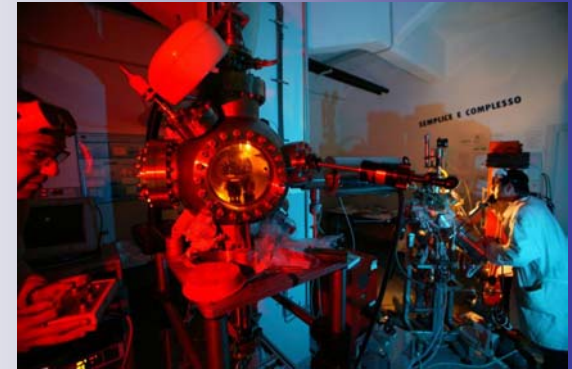
Superconducting fault current limiter fabricated at LAMIA for CESI SpA



Superconducting resonator fabricated at LAMIA for ESAOTE SpA



Thin films of superconducting materials - MgB_2 with extremely high upper critical fields



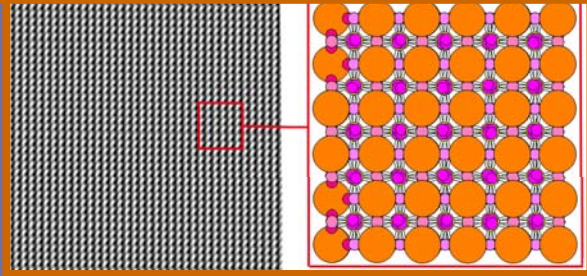
Spin-off company for MgB_2 :
Columbus Superconductors srl:

Km length MgB_2 superconducting tapes and wires

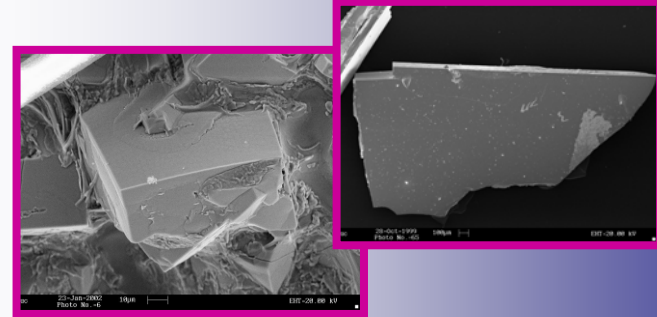


Materials processing

Synthesis of superconducting oxides
Structural refinement and HRTEM analysis



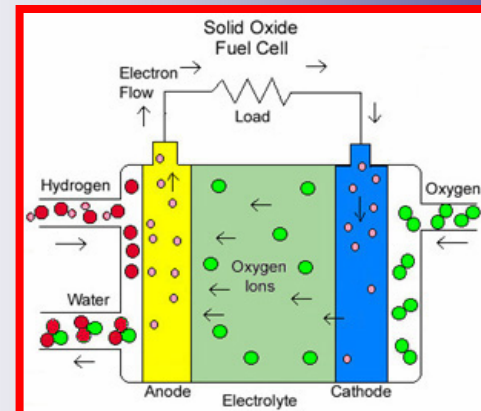
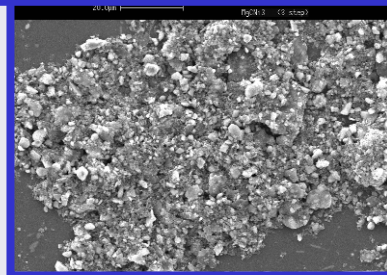
Single crystal growth of
superconducting
and magnetic oxides



HPHT Combustion
synthesis
of nitrides



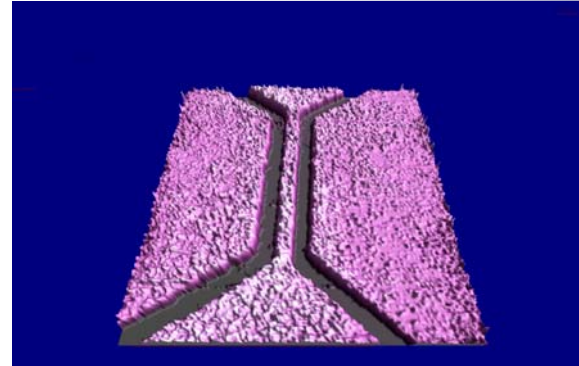
Mechanical alloying
of metallic and ceramic
nanopowders



Synthesis of intermetallic alloys
for hydrogen storage
and ceramics for fuel cells

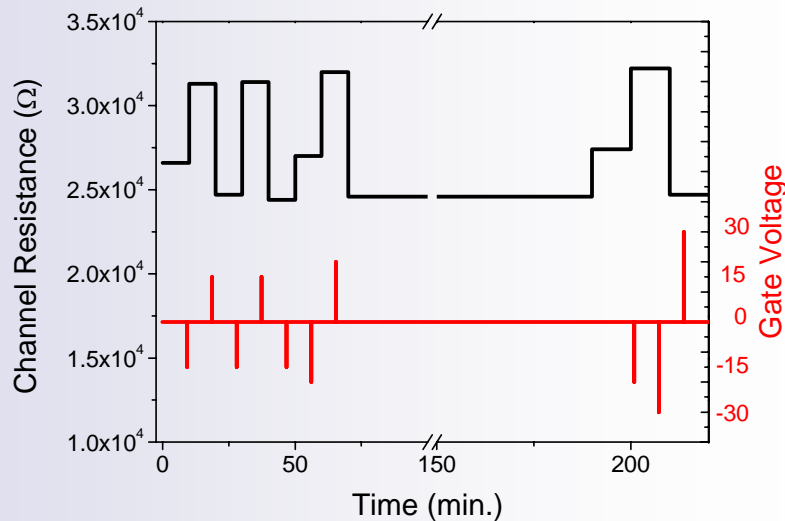
Oxide Electronics: new materials and nanodevices

Field Effect Nanotransistors on Functional Oxides

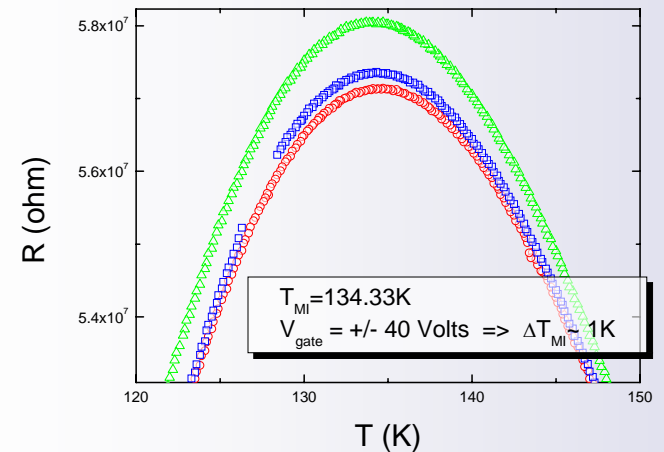


Channel dim: $0.7 \mu\text{m} \times 8 \mu\text{m}$

Ferroelectric Memories



Colossal Magnetoresistance based devices

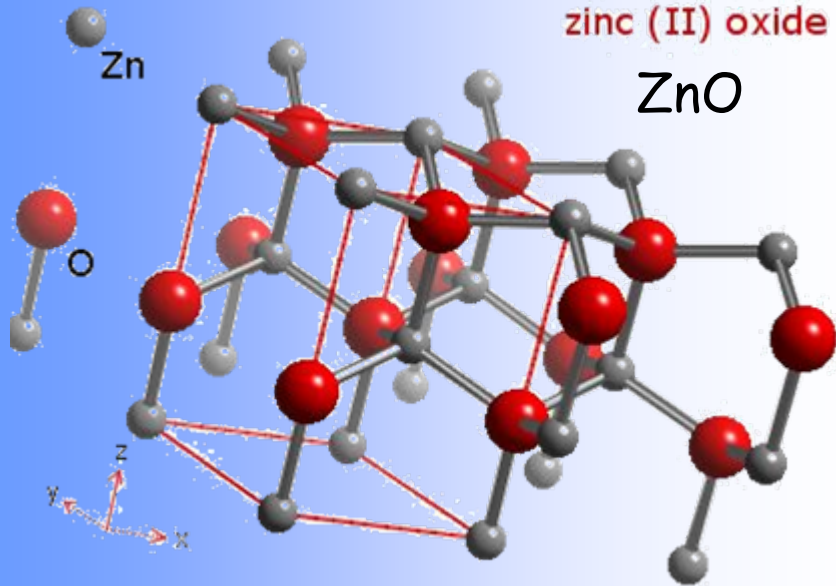


Outline

- Transition metal oxides
 - Perovskite
 - Wurzite
- Field effect geometries
 - Traditional
 - Stacked
 - Back Gate
 - Side Gate
 - Ferroelectric
 - Stacked
 - Local (AFM)
- Experiments
 - Oxide Semiconductor
 - Manganites
 - Superconductor

Transition Metal oxides

Wurzite

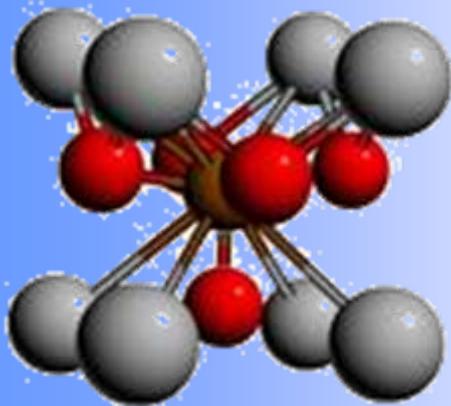


Hexagonal

Lattice parameters
 $a=3.24 \text{ \AA}$, $c=5.19 \text{ \AA}$

- Transparent semiconductor
- High mobility
- Wide-band gap
- Doped with magnetic ions (Co, Mn...): dilute magnetic semiconductors

Perovskite



A: Alkaline Earth
B: Transition Metal
Lattice Parameter
 $(3.9 \pm 0.1) \text{ \AA}$

(Pseudo)cubic

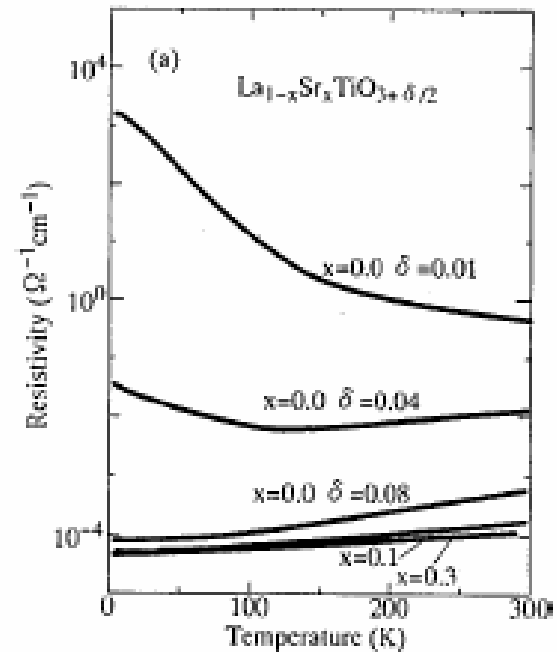
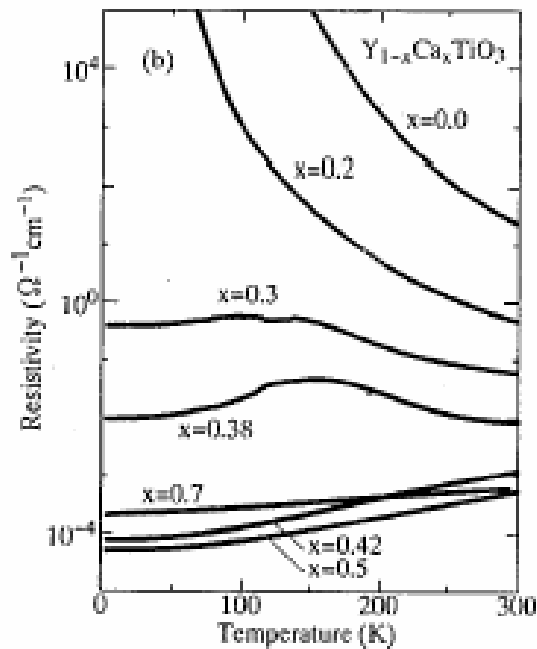
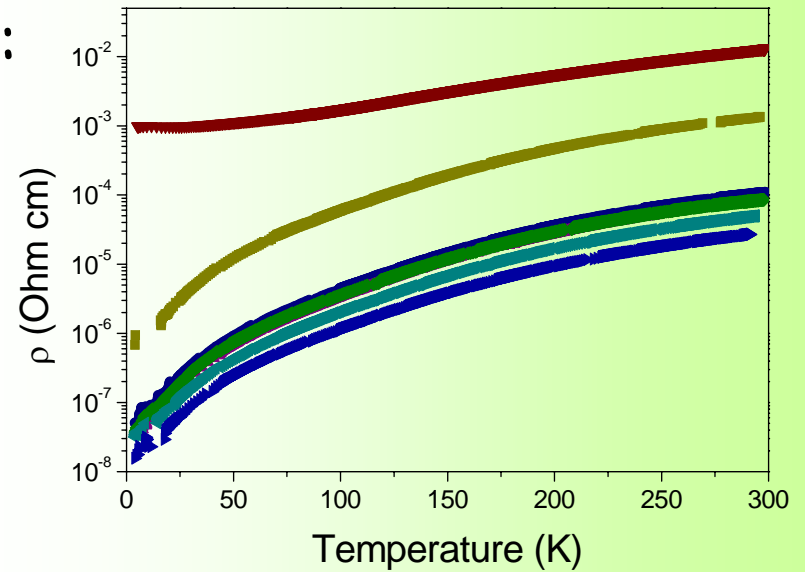
Many physical properties depending on cations

- High T_c superconductivity
- Ferroelectricity
- Ferromagnetism, Colossal Magnetoresistance
- Semiconductors, Insulators

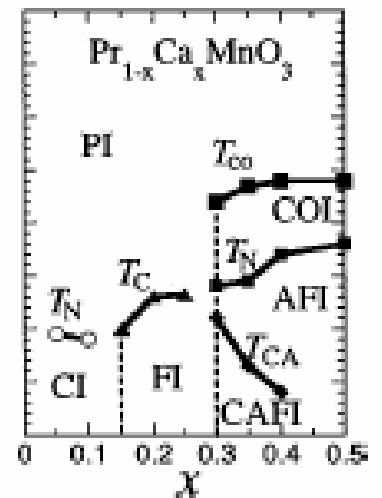
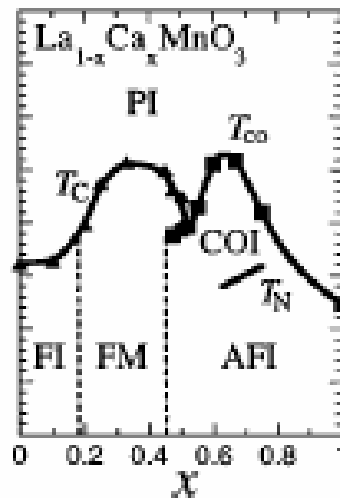
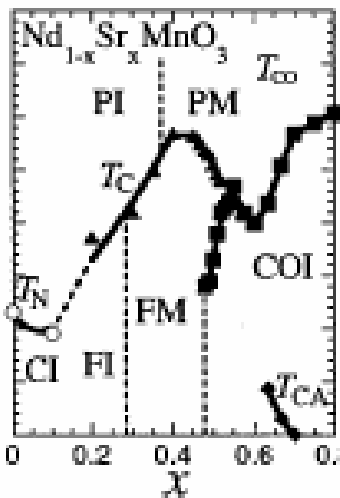
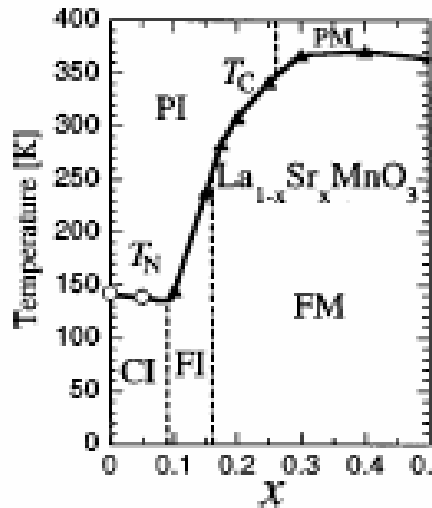
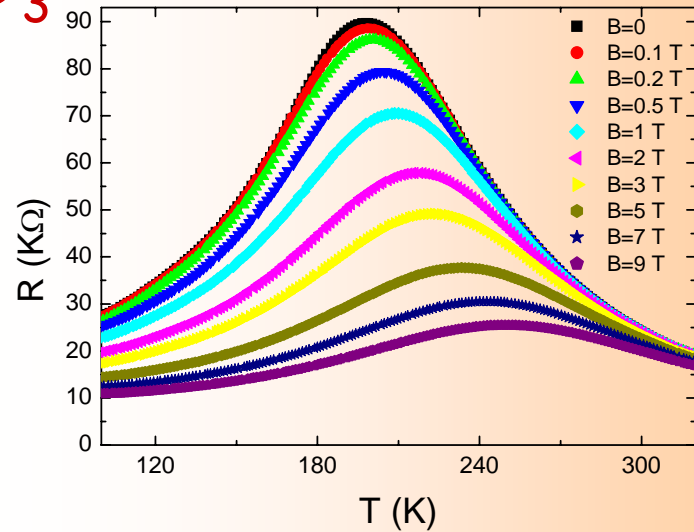
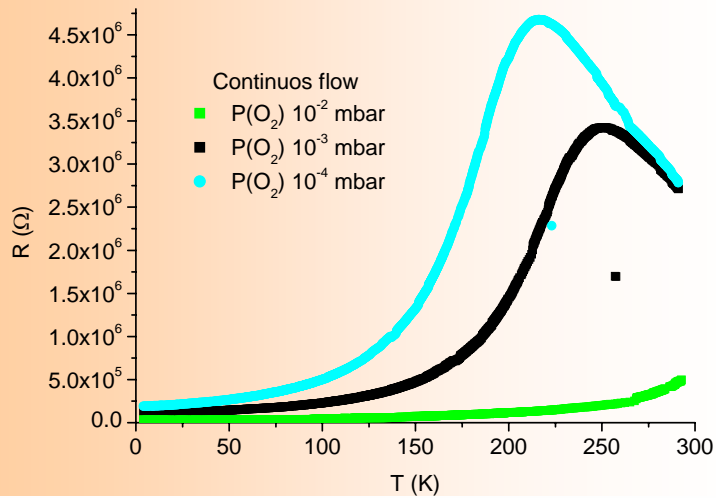
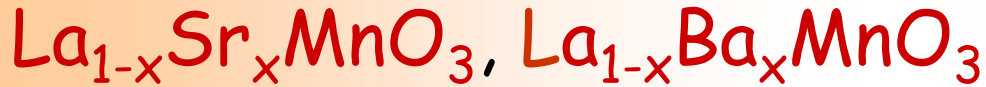
Dielectrics and semiconductors:

SrTiO_3 , LaVO_3 , ZnO

M-I transition in titanates

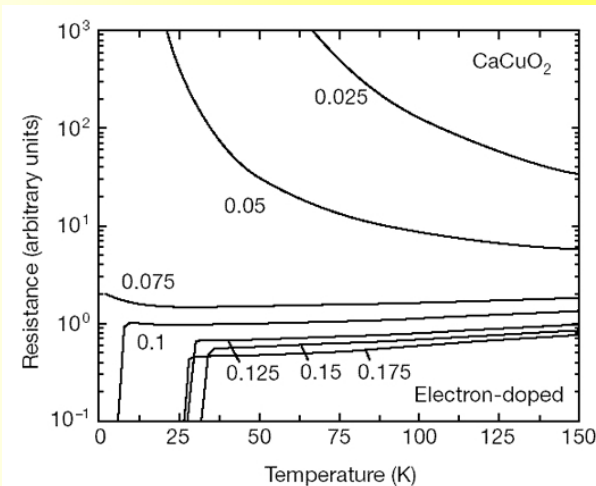
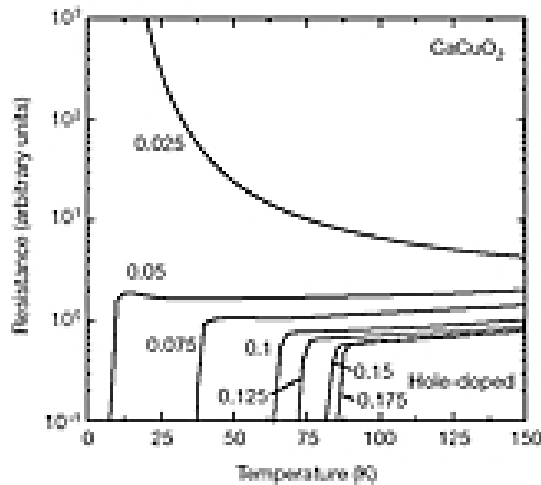
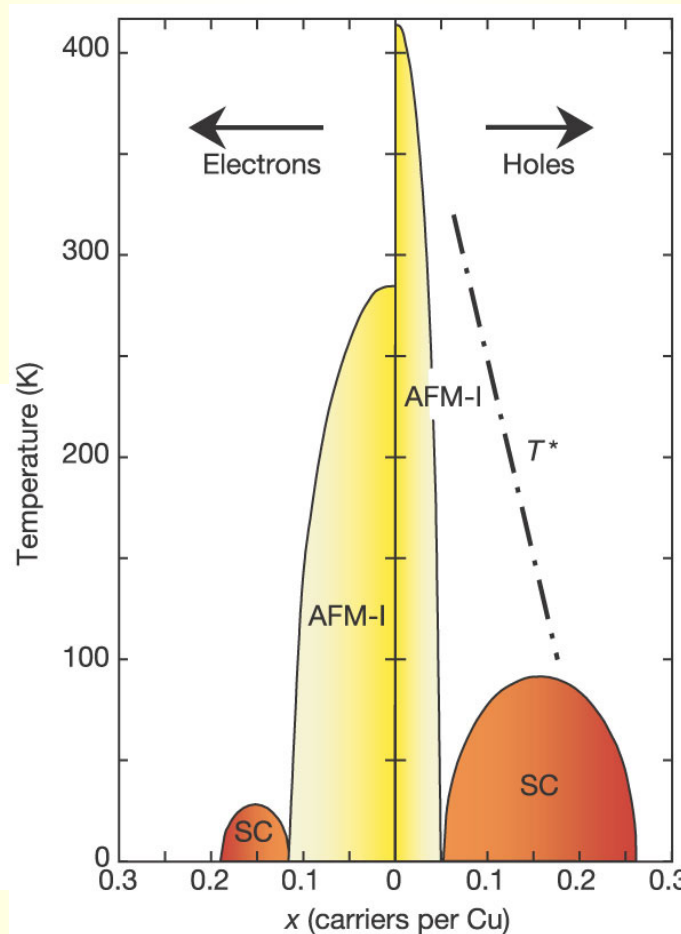
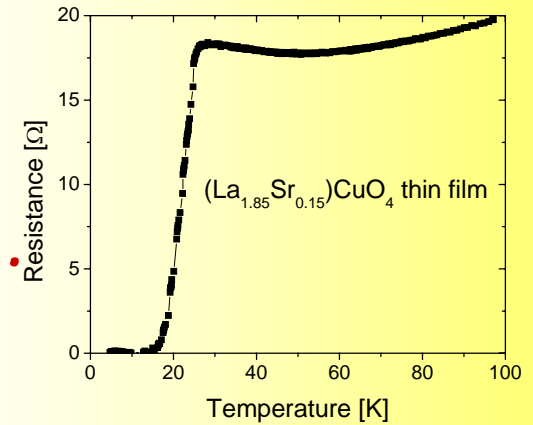


Colossal magnetoresistance:



Superconductivity:

YBCO, LaSCO, infinite layers...



Properties are controlled by:

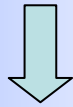
n **Band filling factor** \rightarrow proportional to the charge

W **Band width** \rightarrow proportional to d and p orbital overlapping

How to change n and W ?

**BANDWIDTH
CONTROL**

Cell deformation



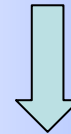
Orbital overlapping

Isovalent atomic substitution
(different radius)

Pressure

FILLING CONTROL

Fermi level variation



Eteroivalent atomic substitution

Field effect

Problem: the phase diagram depends not only on the carrier concentration but also on the lattice structure; chemical doping affects both carrier concentration and lattice structure and it is very difficult to discriminate between these two contributions.

Field effect tunes the carrier concentration only, thereby it is a powerful tool to study this correlated system

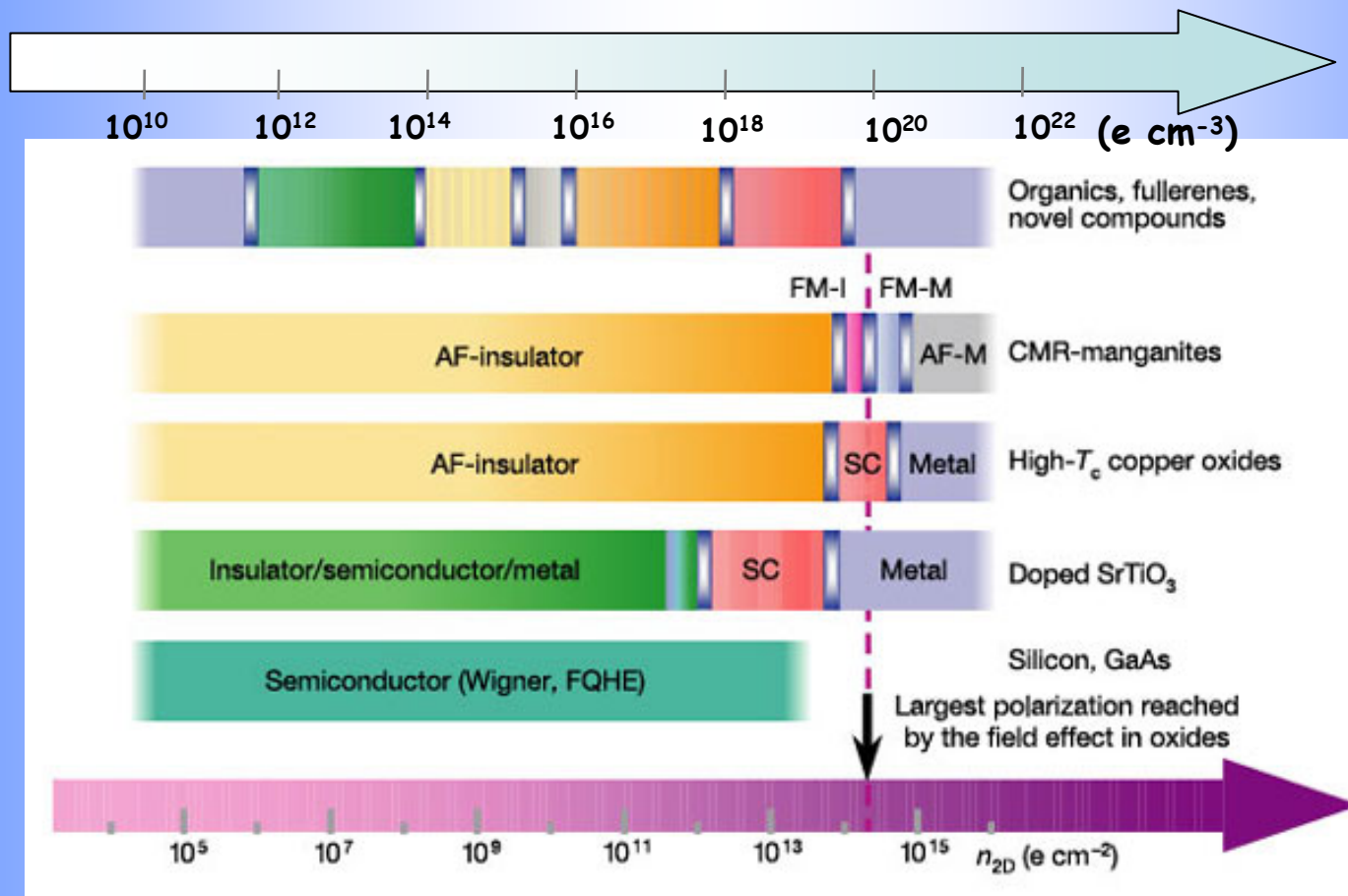


Illustration of the zero-temperature behaviour of various correlated materials as a function of charge density. Silicon is shown as a reference. The examples for high- T_c superconductors and for colossal magnetoresistive (CMR) manganites reflect $\text{YBa}_2\text{Cu}_3\text{O}_{7-x}$ and $(\text{La,Sr})\text{MnO}_3$, respectively.

AF, antiferromagnetic; FM, ferromagnetic; I, insulator; M, metal; SC, superconductor; FQHE, fractional quantum Hall effect; Wigner, Wigner crystal.

Electric field effect in correlated oxide systems

C. H. Ahn, J.-M. Triscone and J. Mannhart

Nature 424, 1015-1018 (28 August 2003) doi: 10.1038/nature01878

Many of interesting physical properties in these material occur at 10^{19} - 10^{21} e-/cm³
(for 100 nm film => 10^{14} – 10^{16} e/cm² => 10 – 1000 μ C/cm²)
Very high q value!

High polarization
Ultrathin films

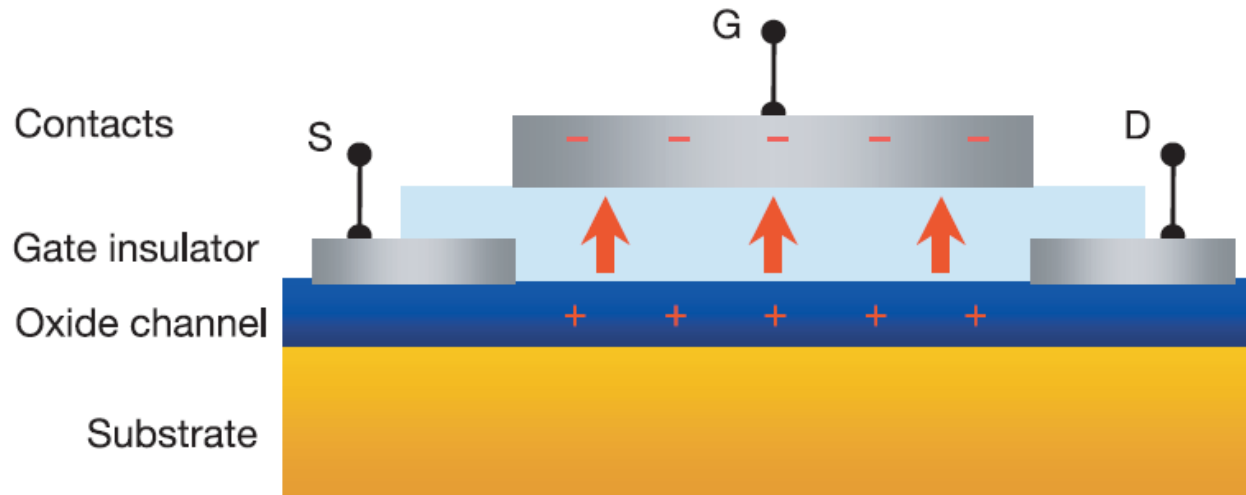


Figure 2 Cross-section of a typical sample geometry used for field-effect studies.
S, source; G, gate; D, drain.

The characteristic width of accumulation or depletion layer is given by the electrostatic screening length

Thomas-Fermi for metal $k_{TF} = \sqrt{\frac{3ne^2}{\epsilon_0\epsilon_r E_F}} \approx 1 \text{ \AA}$

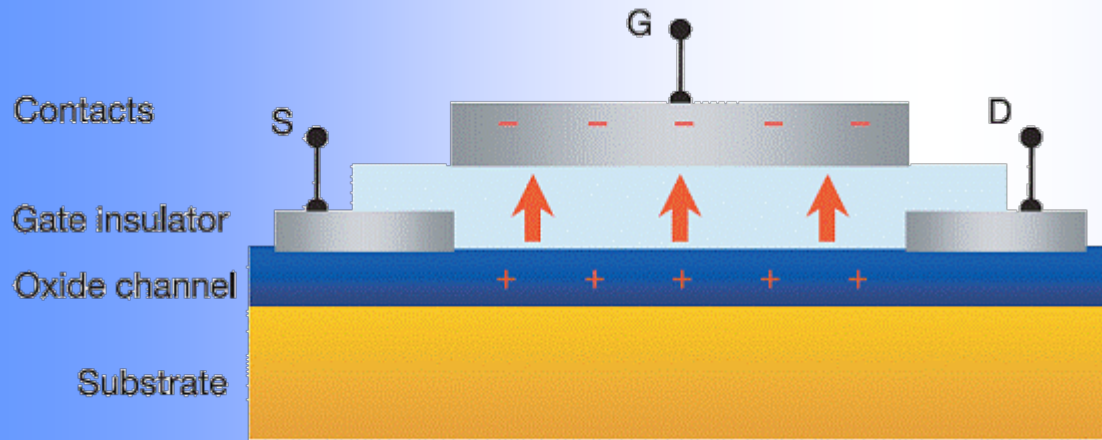
$$\lambda_{TF} = \frac{2\pi}{k_{TF}} = \sqrt{\frac{4\pi^2 \epsilon_0 \epsilon_r E_F}{3ne^2}}$$

Debye for semiconductors $\lambda_D = \sqrt{\frac{kT\epsilon_0\epsilon_s}{e^2 n_{ext}}} \approx 10 \text{ nm}$

Lower carrier density \rightarrow larger λ

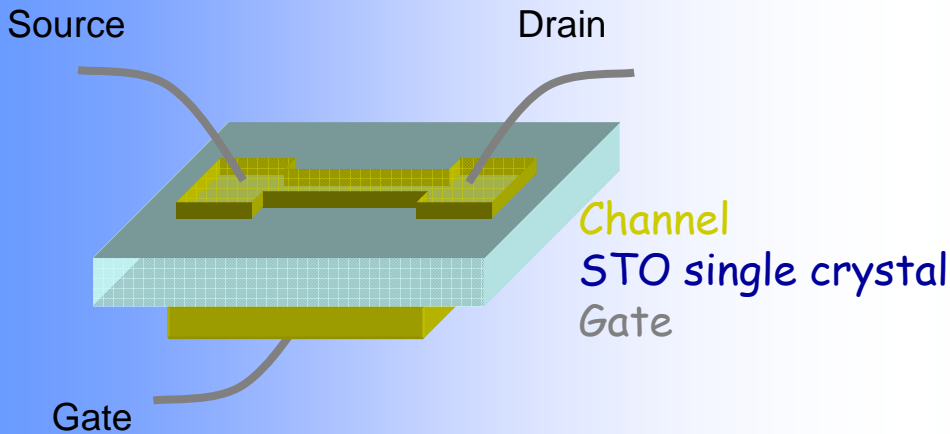
Debye length at room temperature			
$N(e/cm^3)$	$\epsilon_r=300$	$\epsilon_r=100$	$\epsilon_r=10$
$10^{20} (e/cm^3)$	2.0 nm	1.2 nm	0.38 nm
$10^{19} (e/cm^3)$	6.5 nm	3.8 nm	1.2 nm
$10^{18} (e/cm^3)$	20 nm	12 nm	3.8 nm

Field effect devices: Stacked Geometry



MIS heterostructure Metal-Insulator-Semiconductor

- Growth of the dielectric layer on the channel
- Compatibility problems
- Leakage

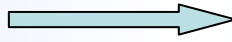


Back gate geometry

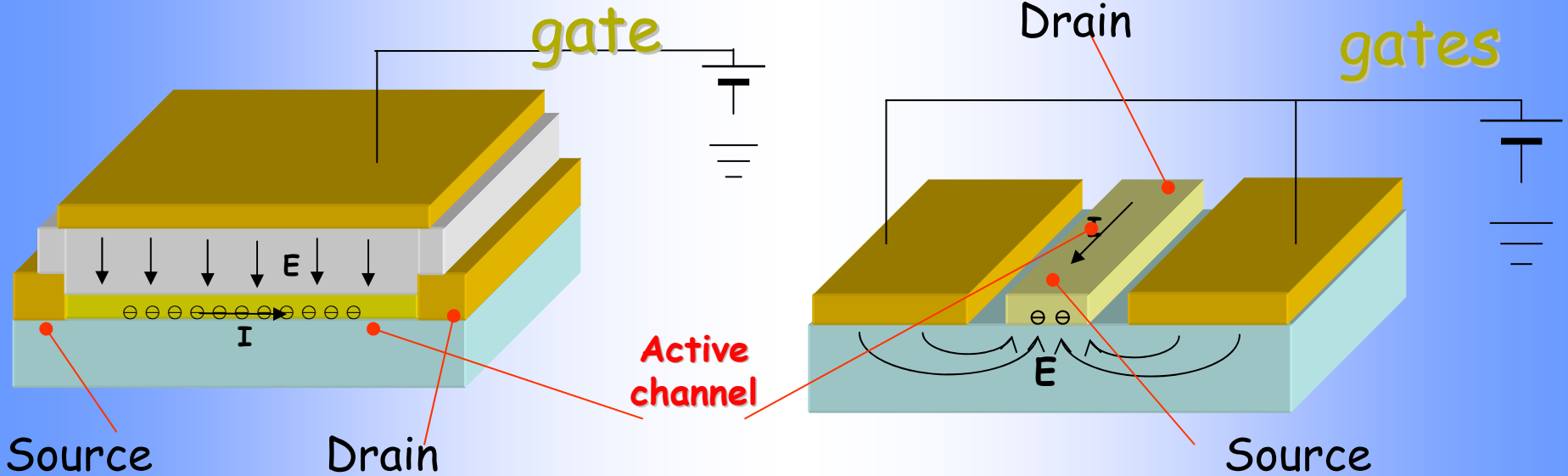
- Very good dielectric properties of the oxide (single x-tal)
- Very thick → High voltage

Side gate devices

Planar Geometry

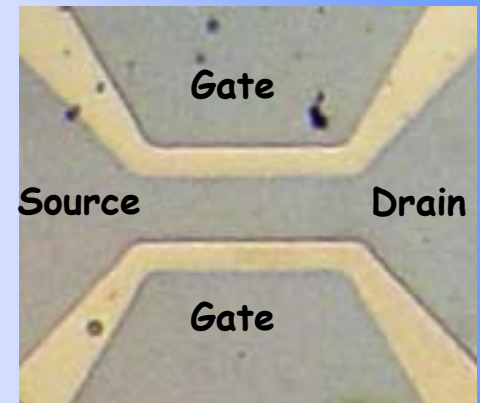


Side Gate Geometry



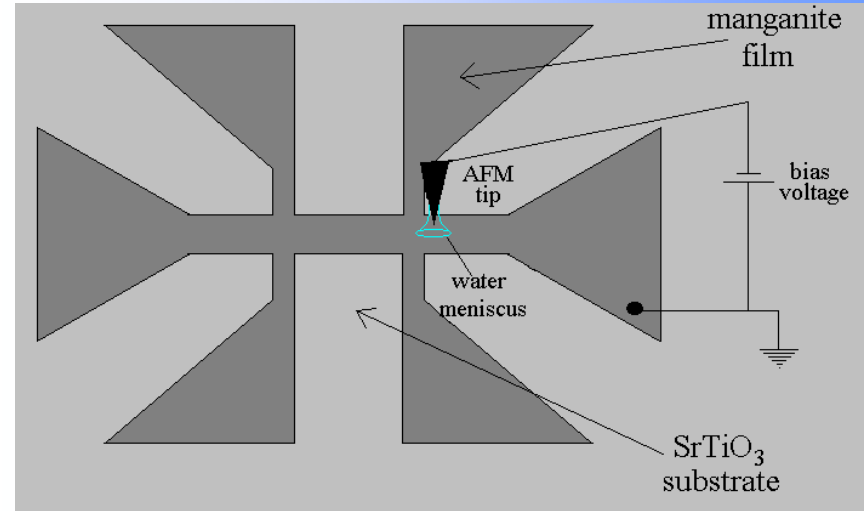
Advantages of the side gate geometry

- Easy: 2-layers structure (film/substrate)
- High quality substrates \rightarrow Best Dielectric Properties
- Low voltage required
- Possibility to study the surface by Scanning Probe Microscopy

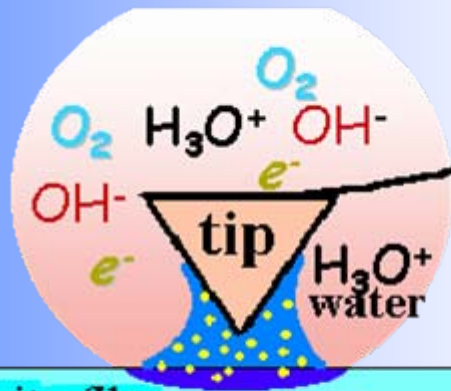


Side gate field effect devices fabrication by AFM

First step: patterning by **optical lithography** and wet etching in 10-20 μm wide crossing channels with bond pads



*Conducting silicon
 W_2C coated tip
0.12N/m*



manganite film

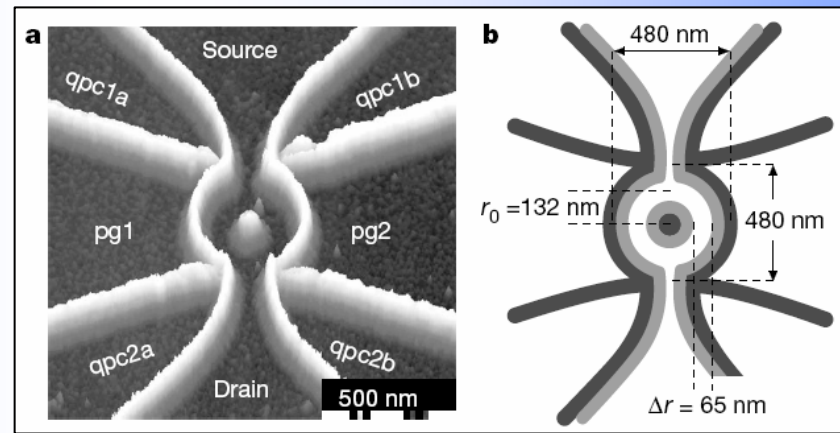
STO substrate

Second step: sub-micron patterning by **Atomic Force Microscope anodization**: the AFM biased tip triggers a **local chemical and morphological transformation**.

Nanoxidation of silicon

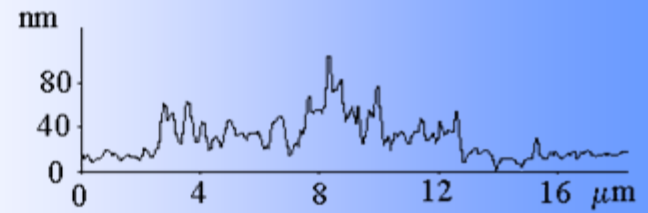
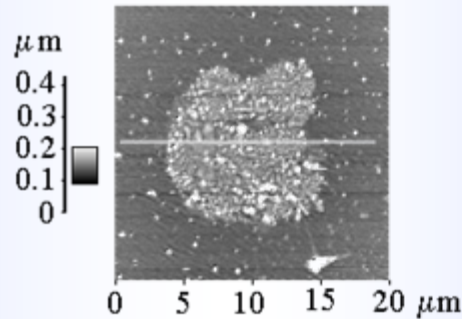
J.A.Dagata, et al., Appl. Phys. Lett. **56**, 2001 (1990)

•Nanoscale GaAs/AlGaAs heterostructures

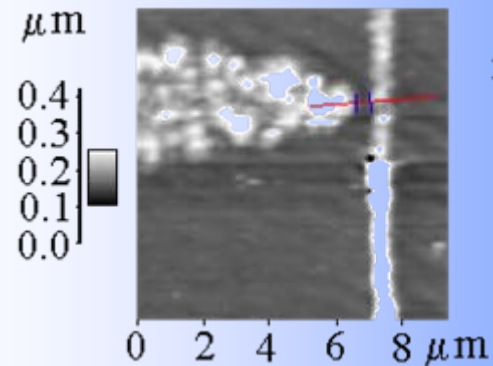


Local "anodic oxidation" of oxides:

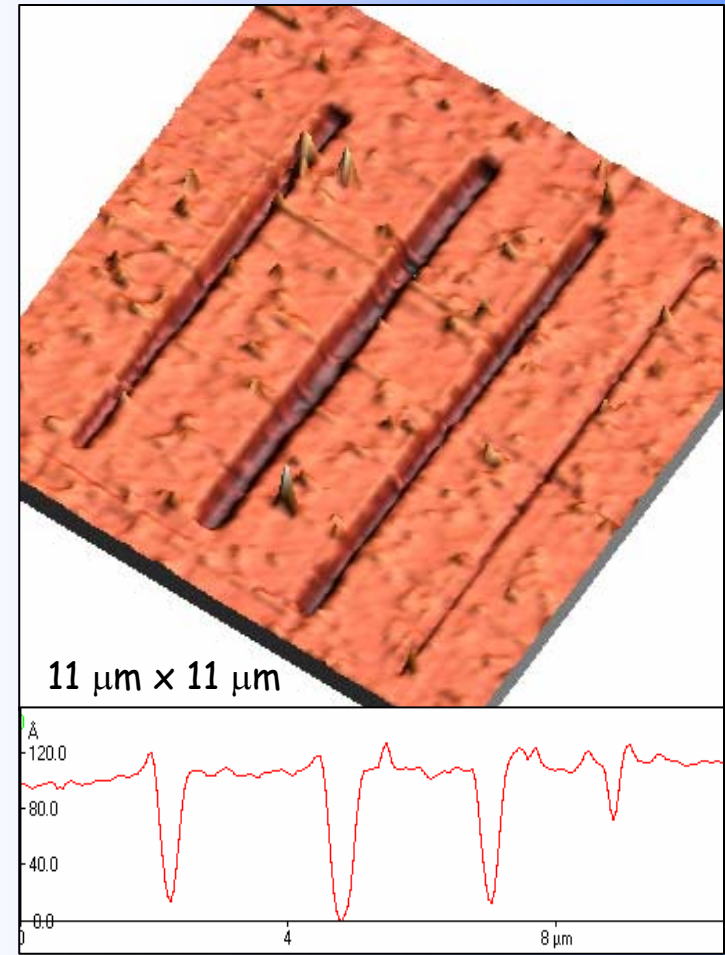
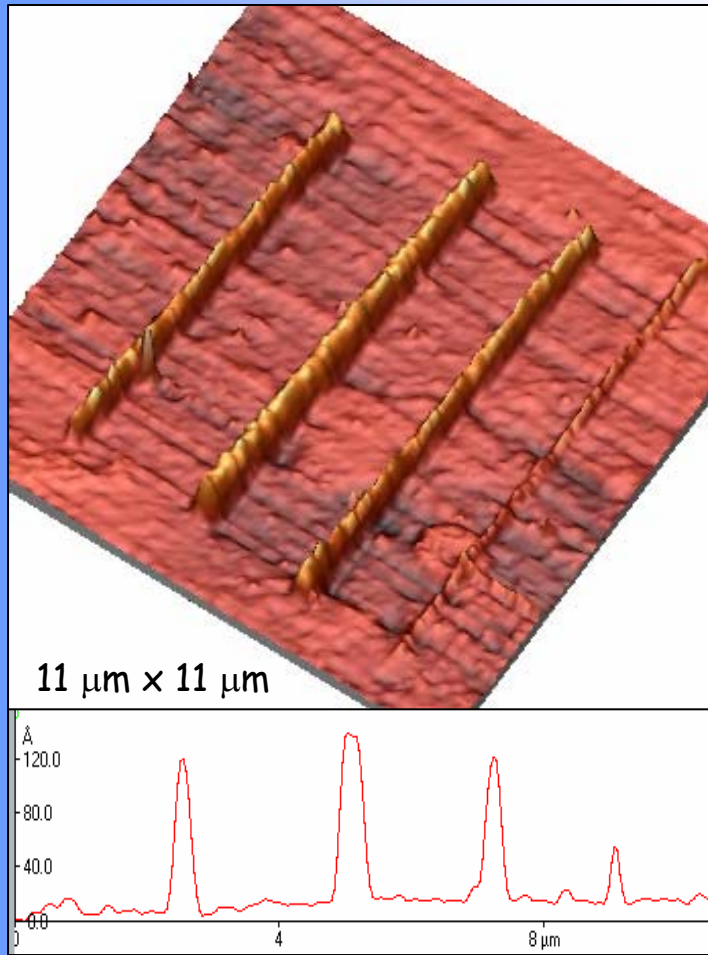
The modified regions are swollen, porous and electrically insulating



Fabrication of **constrictions** as narrow as 40 nm.

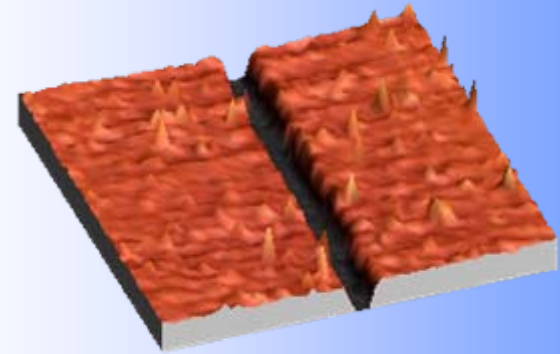
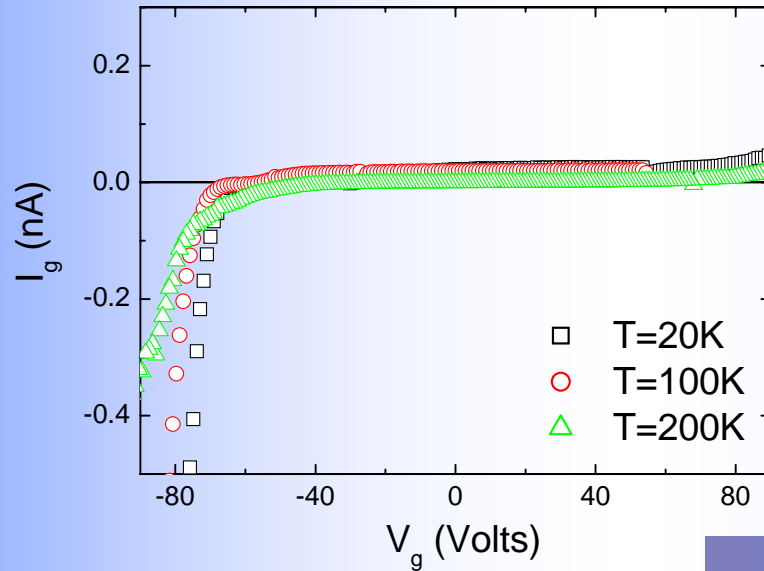


Modified regions are selectively etched in HCl solution

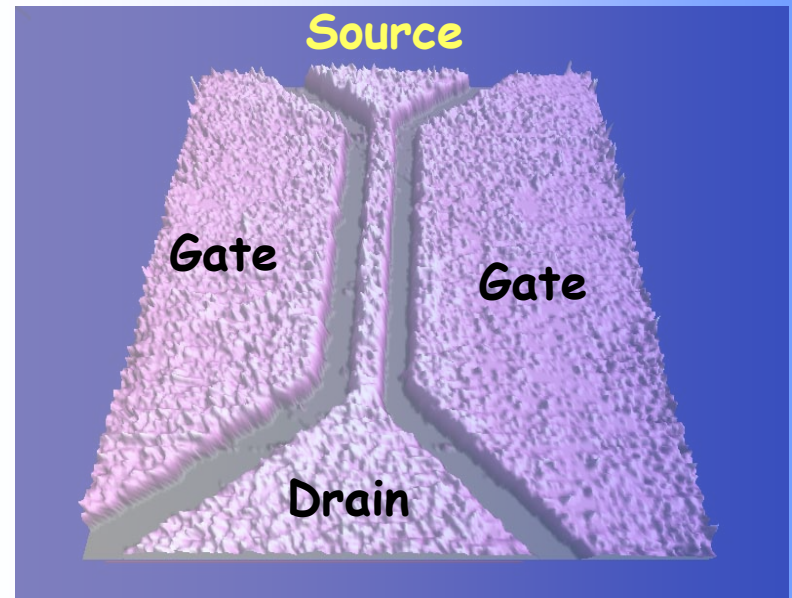


Voltage controlled etching depth !!!

Etched sub-micron wide insulating barriers can sustain **applied voltages up to ± 80 Volts without appreciable leakage (< 100 pA).**



Side gate field effect devices by AFM

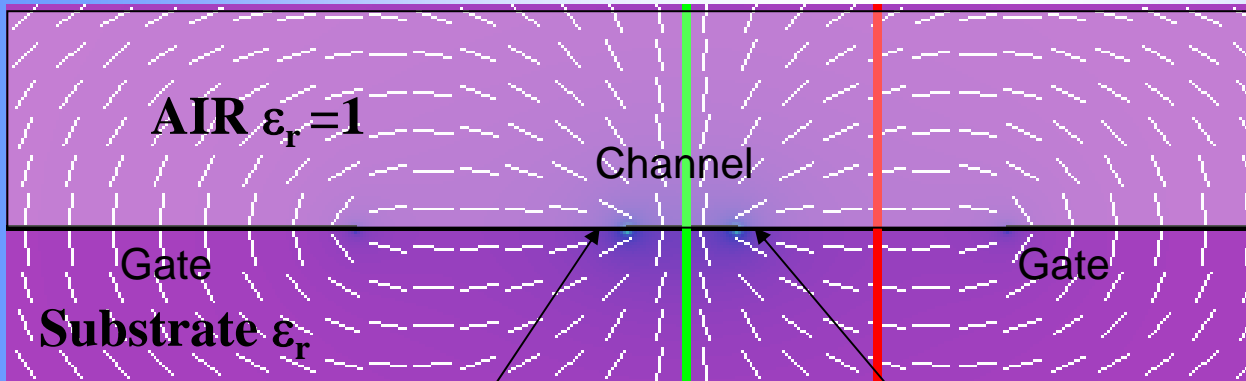


Electric field profile and capacitance calculation

Channel width 600 nm

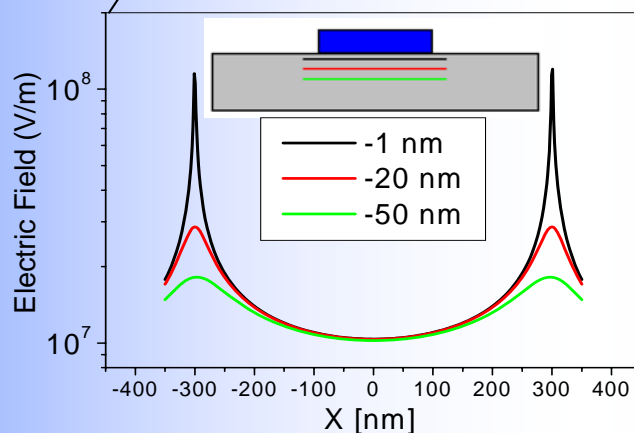
Gap 1200 nm, Thickness 10 nm

Applied Voltage $V = 10V$



Estimated capacitance:

$$C/m = 8.8 * \epsilon_r \text{ pF/m}$$



$V_g = 10 \text{ Volts}$

$$\frac{dn_{sheet}}{dV_g} = \epsilon_r \times 10^{10} (e/cm^2V)$$

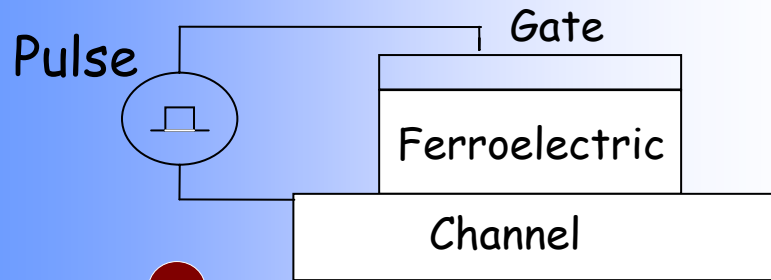
$$\epsilon_r = 25 \text{ (LAO)}$$

$$\rightarrow dn_{sheet} = 2.5 \times 10^{12} (e/cm^2)$$

$$\epsilon_r = 1000 \text{ (STO)}$$

$$\rightarrow dn_{sheet} = 10^{14} (e/cm^2)$$

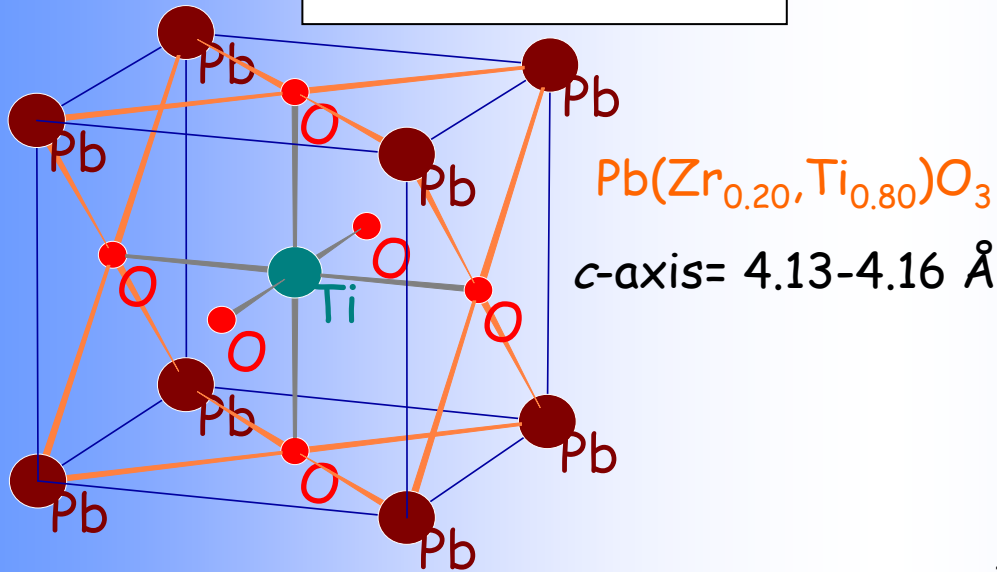
Ferroelectric Field effect



Induced charge proportional to the ferroelectric remnant polarization

Remnant polarization
 $P_r \sim 10\div 60 \mu\text{C}/\text{cm}^2$

Coercive field
 $E_c \sim 100 \text{ kV}/\text{cm}$

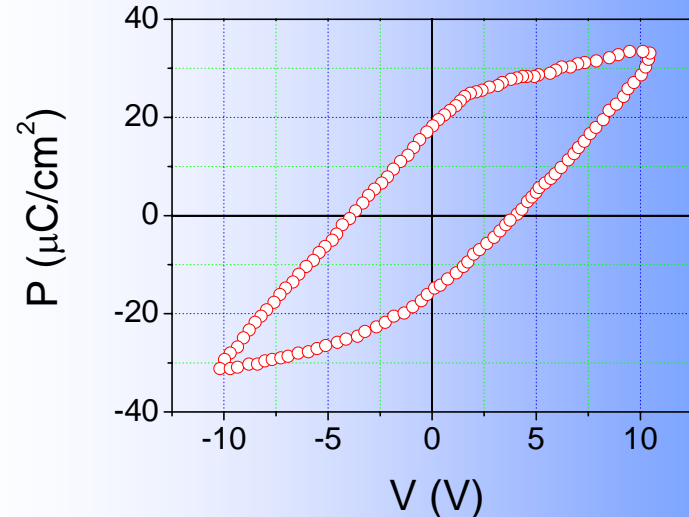


Ferroelectric properties:

$P_r \sim 20 \mu\text{C}/\text{cm}^2$

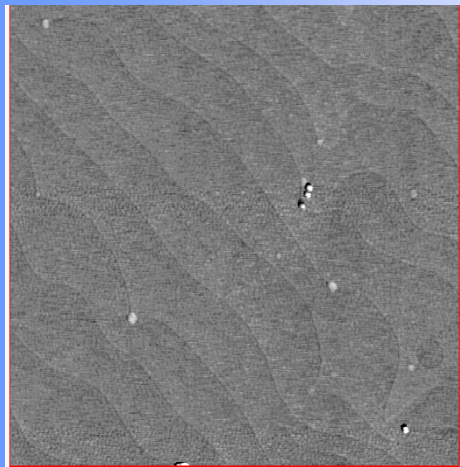
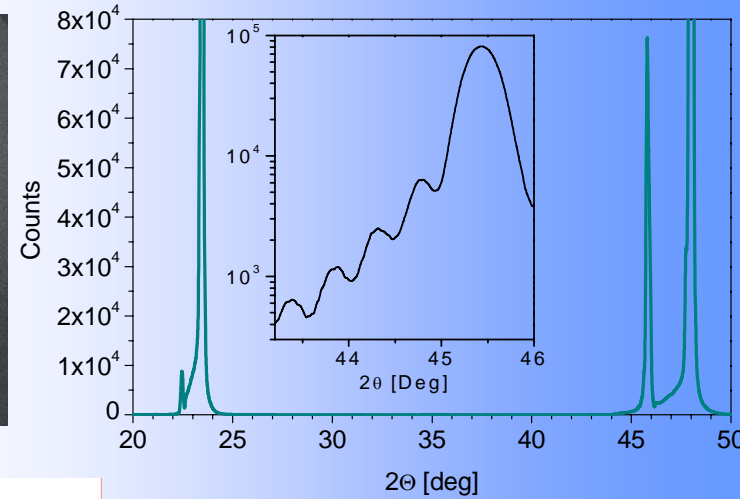
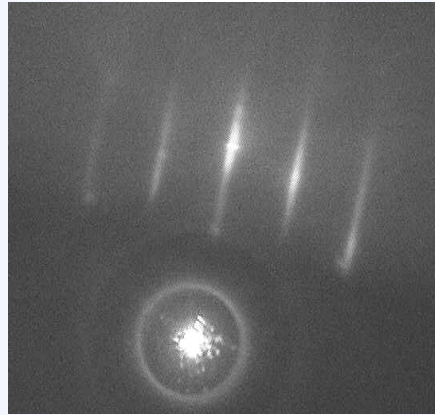
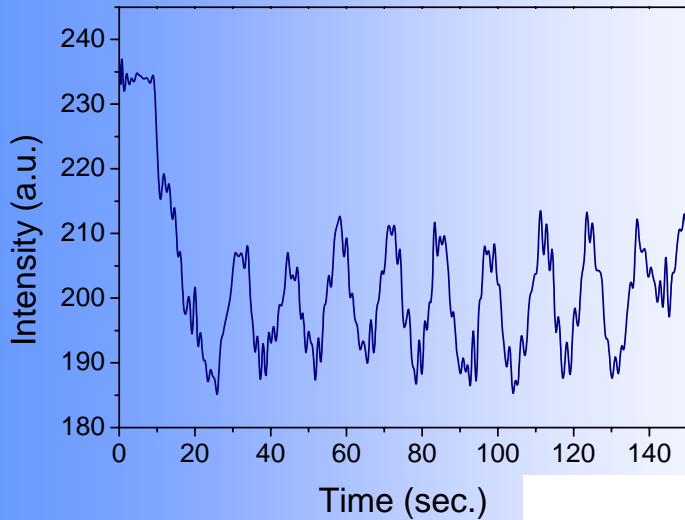
$\sigma \sim 10^{14} \text{ charges}/\text{cm}^2$

- No V applied during measurements
- No leakage
- Only 2 states available



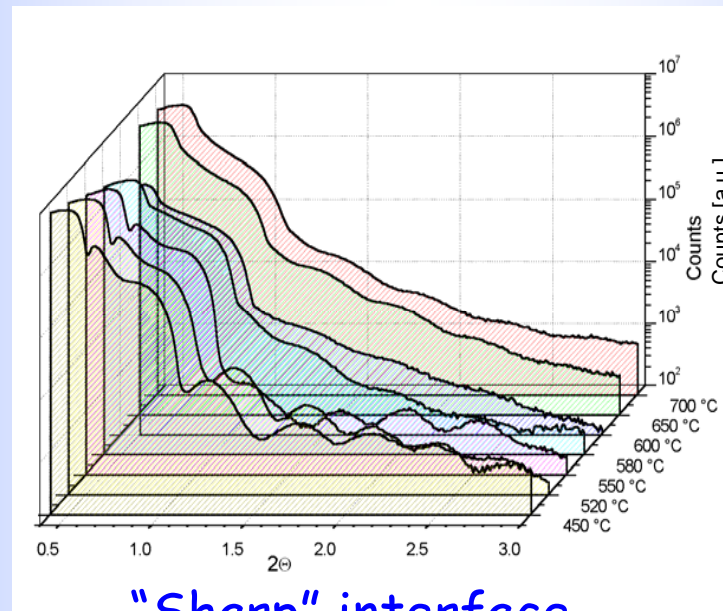
Perovskite films growth and structural properties

Layer by layer growth

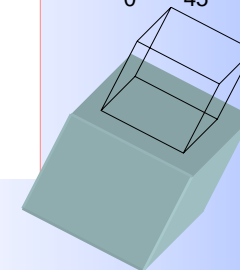
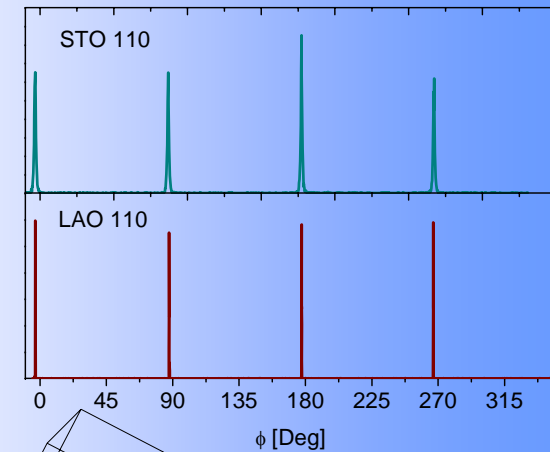


0 2 4 μm

Atomically
smooth surfaces



"Sharp" interface
reflectivity

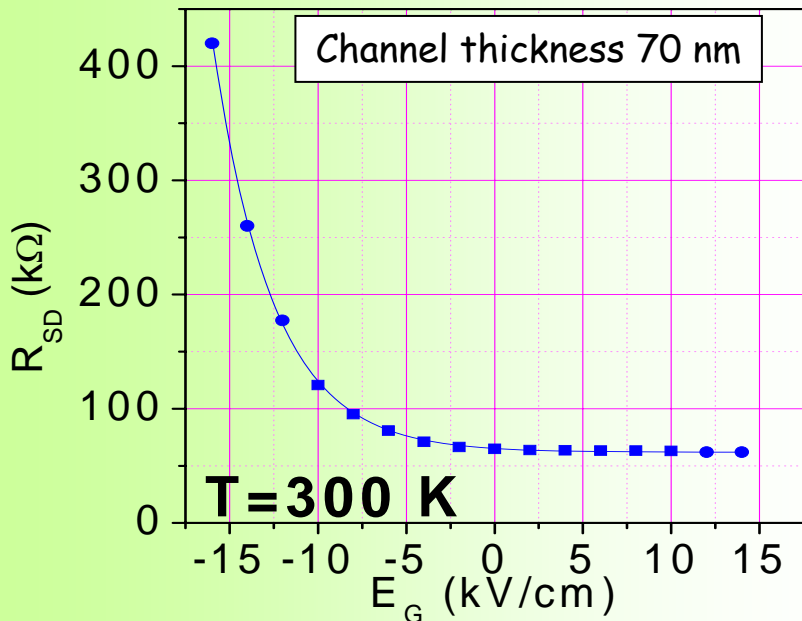
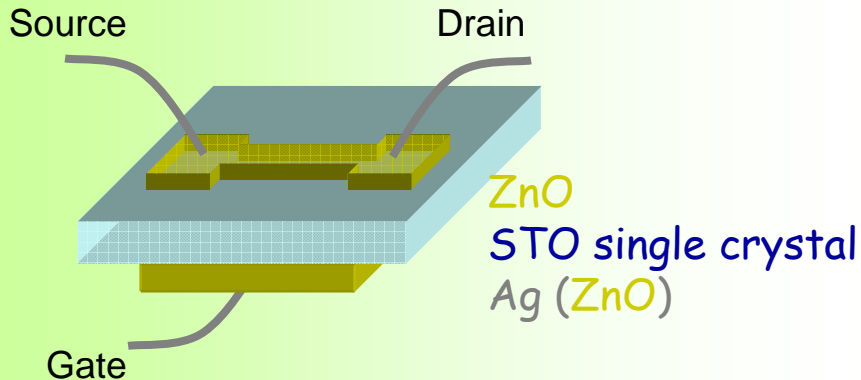


"Cube on cube"
epitaxial growth

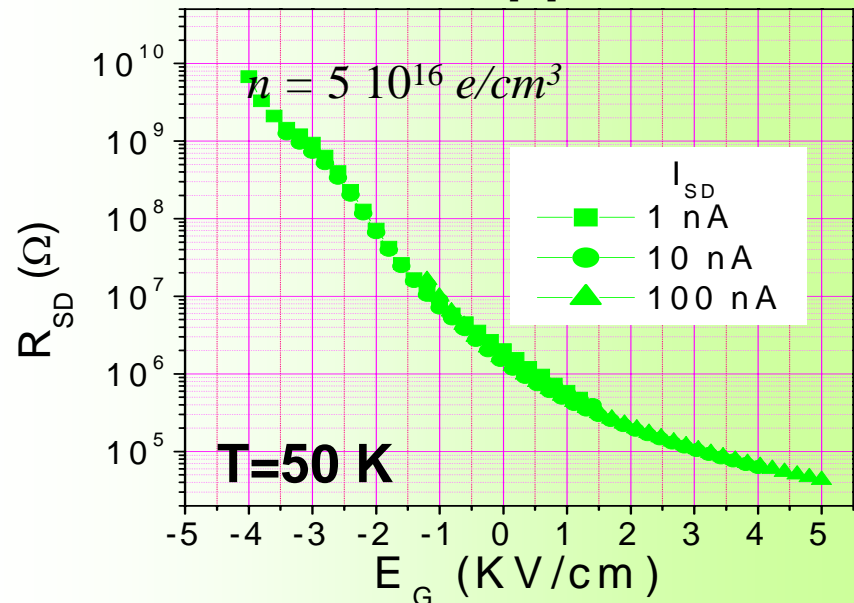
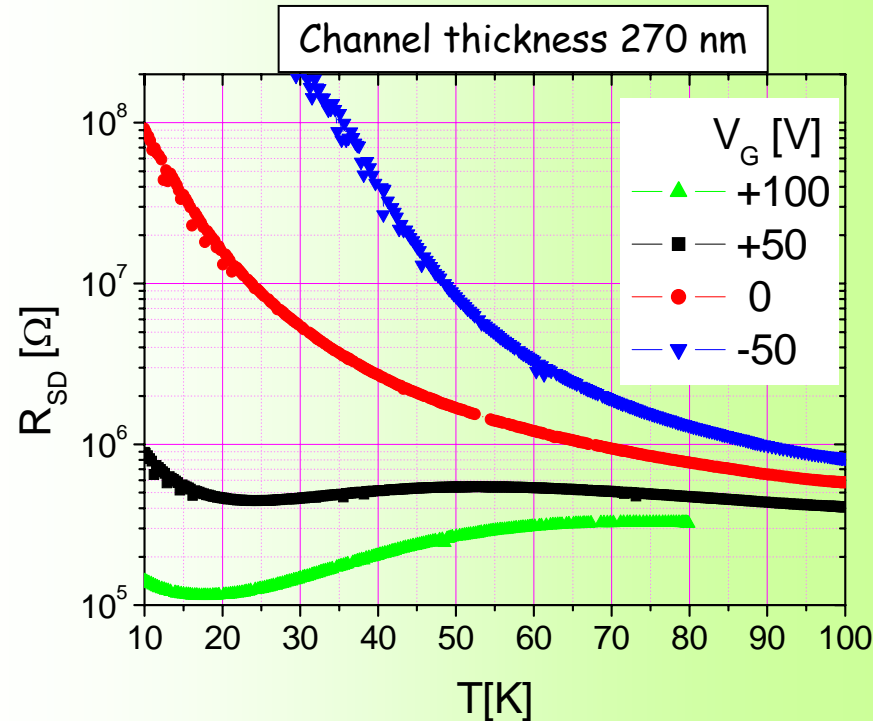
Oxides Semiconductors

Easy case : ZnO Back-gate devices

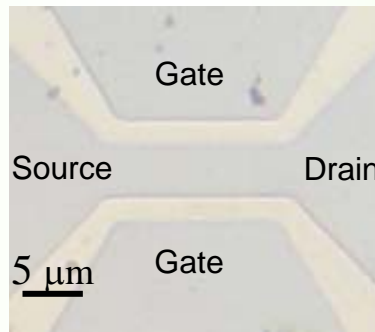
Double side polished $SrTiO_3$ 110 substrate



• More than 5 order of magnitude R_{SD} modulation at 50K

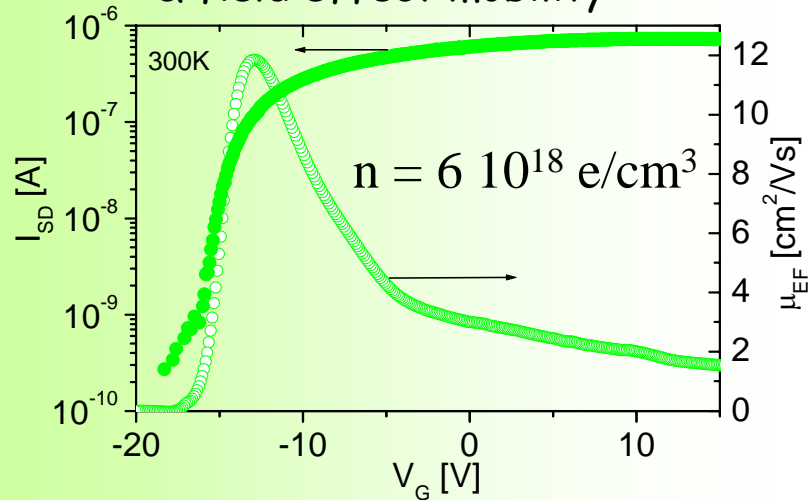


ZnO Side gate devices

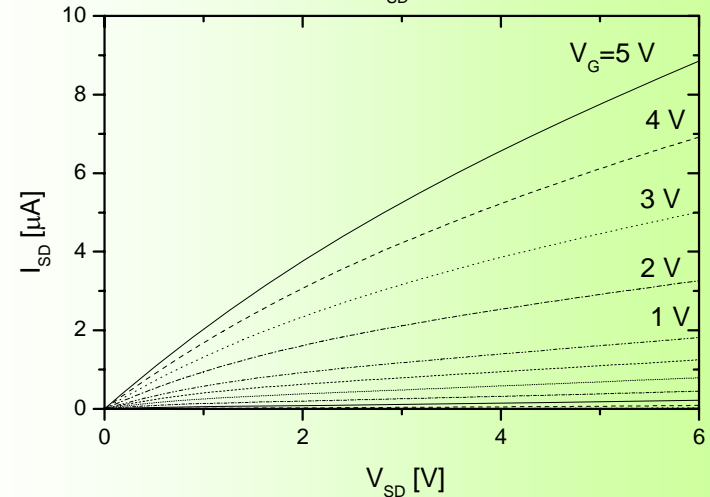
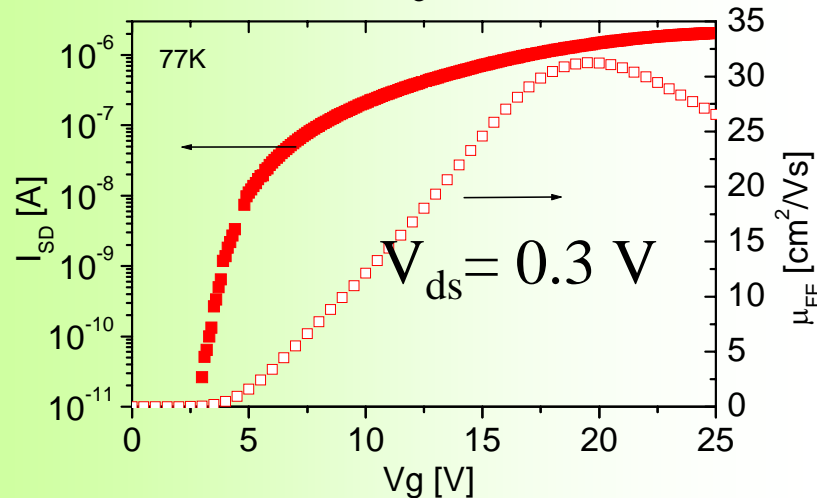
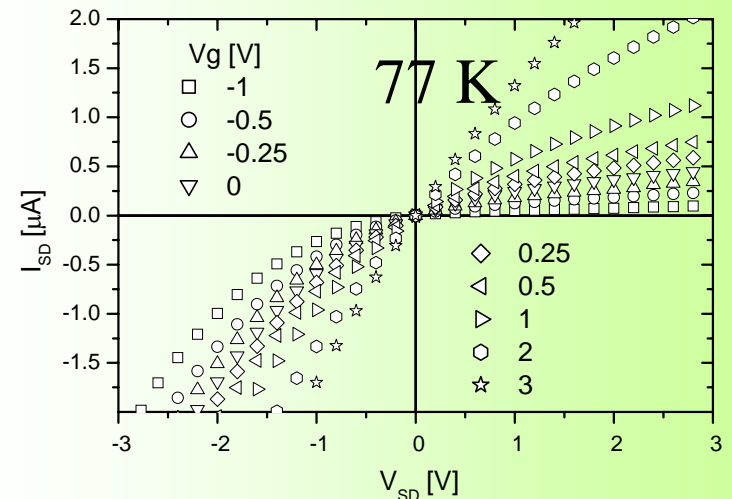


20 nm thick ZnO
film by two-step
method

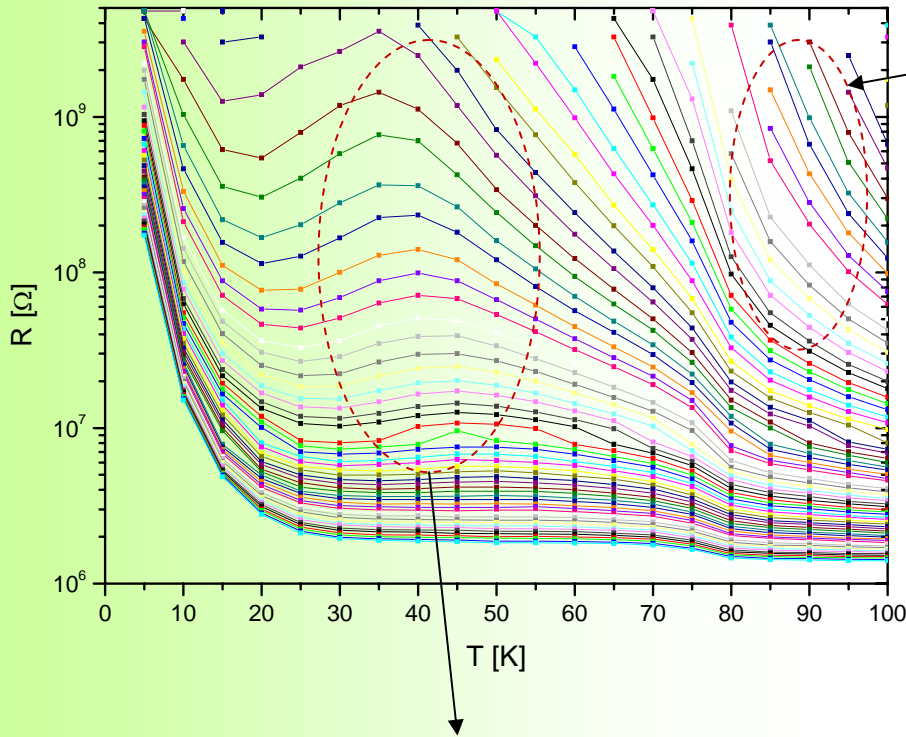
Transfer characteristics & field effect mobility



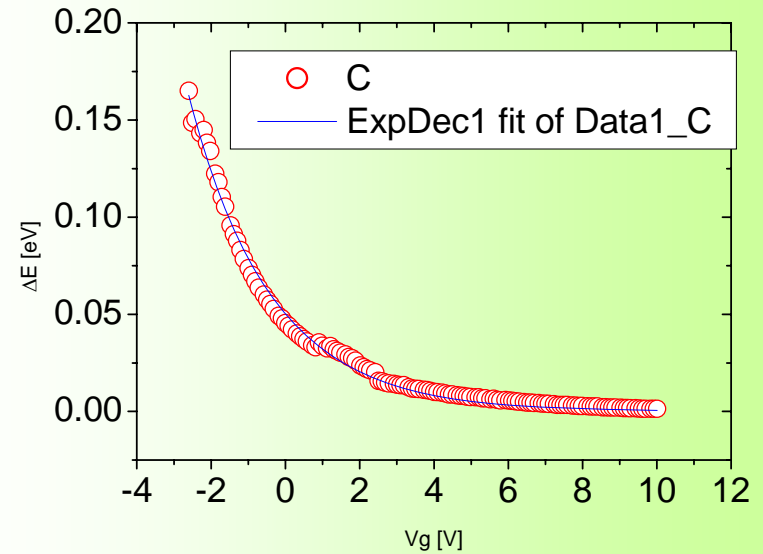
Characteristic curves



Thermal activated behaviour



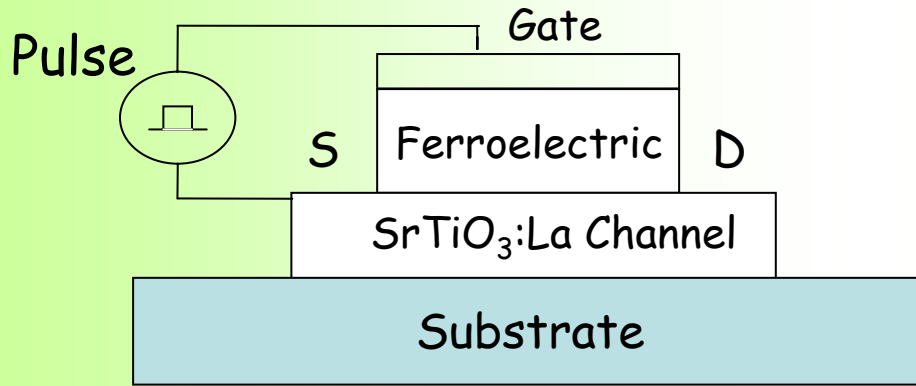
MIT driven ϵ_r of the STO substrate
Competition between T and V
dependences of ϵ_r



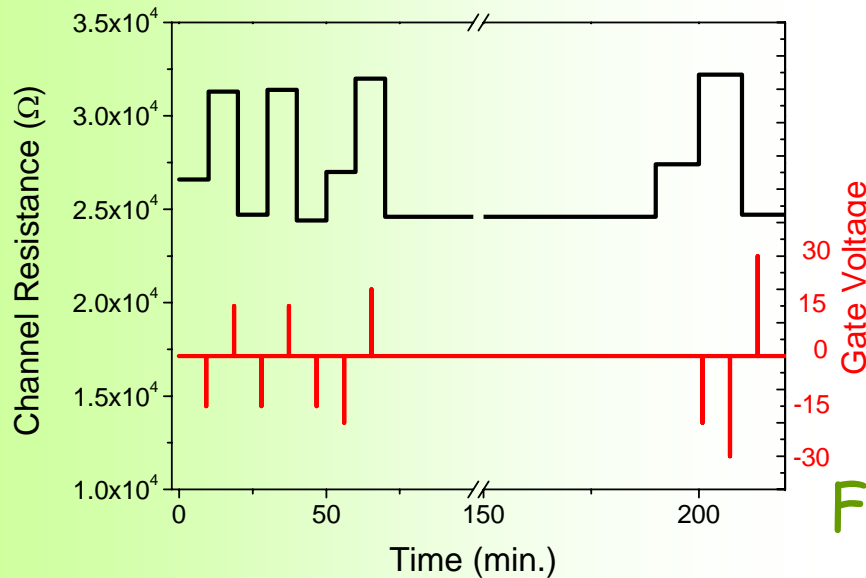
Estimation of the density of state
(impurity band)

$$D(E) \propto 1/(E - E_c)$$

Ferroelectric field effect on SrTiO₃ channel



Time stable 20 % change
in channel resistance
modulated by
polarization pulses



Consistent with
channel thickness
and channel carrier
density

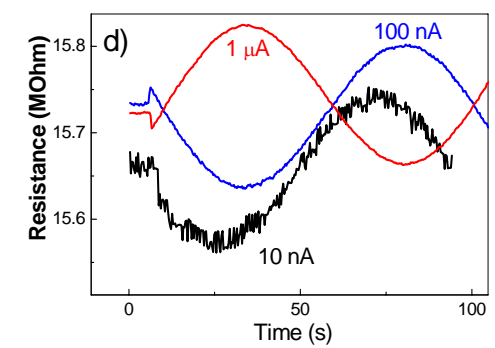
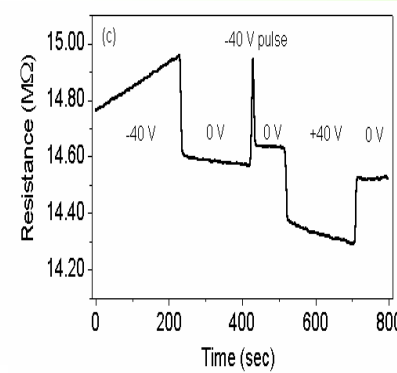
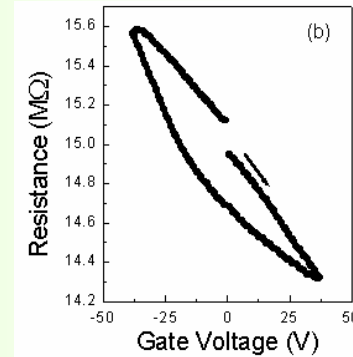
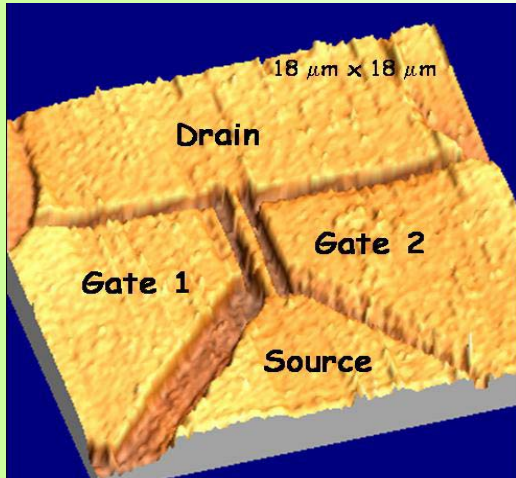


Ferroelectric Field Effect

Strontium titanate resistance modulation by ferroelectric field effect

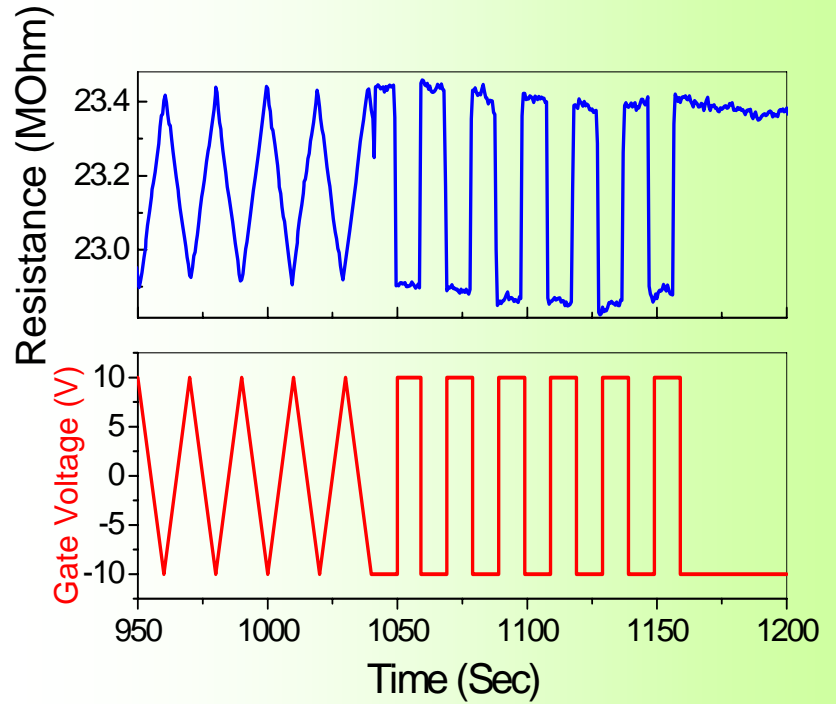
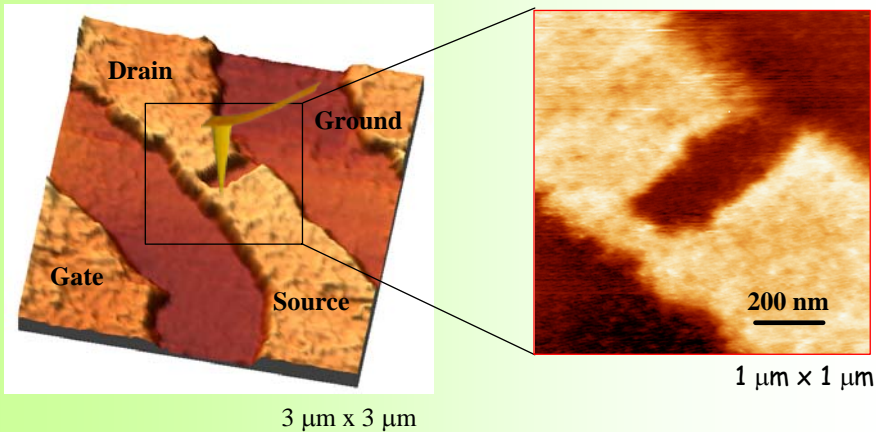
D. Marré, A. Tumino, E. Bellingeri, I. Pallecchi, L. Pellegrino, A.S. Siri,
J. Phys. D: Appl. Phys. 36 No 7 896-900 (2003)

First example of side gate devices (SrTiO_3 on LaAlO_3)

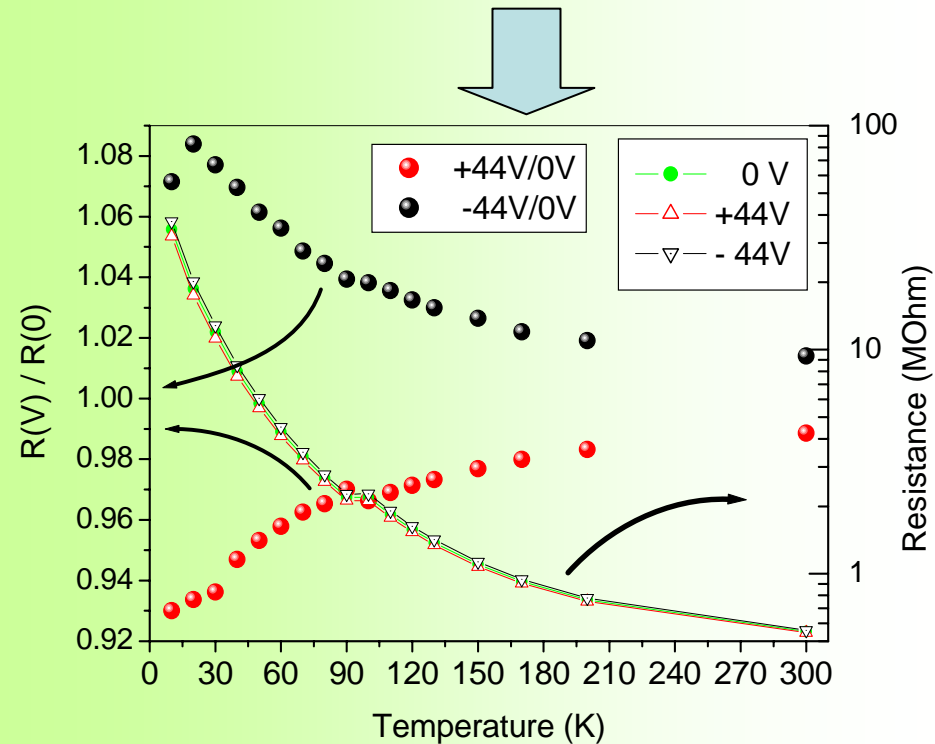
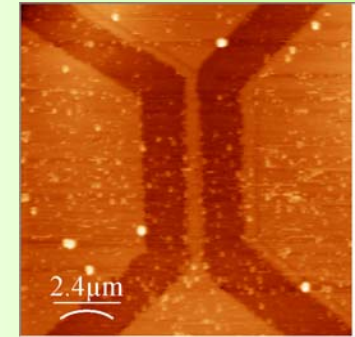
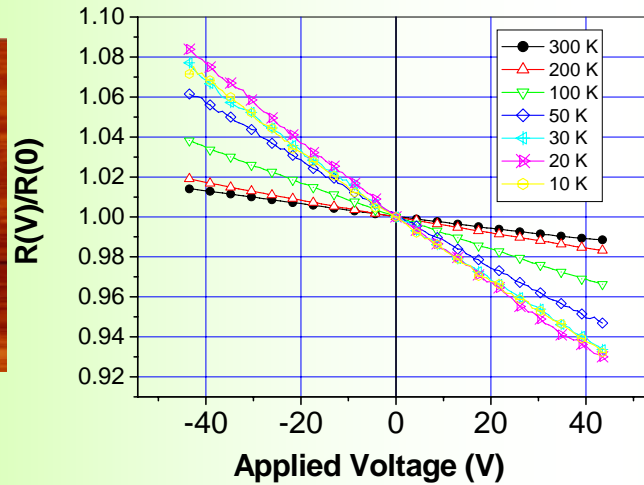
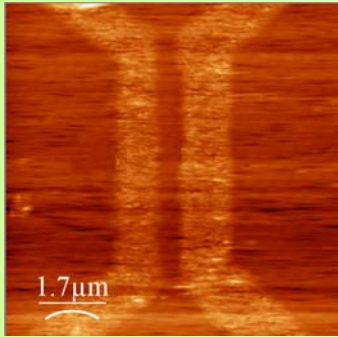


Fabrication of submicron-scale SrTiO_3 devices by an atomic force microscope L. Pellegrino, et al Appl. Phys. Lett. **81**, 3849 (2002)

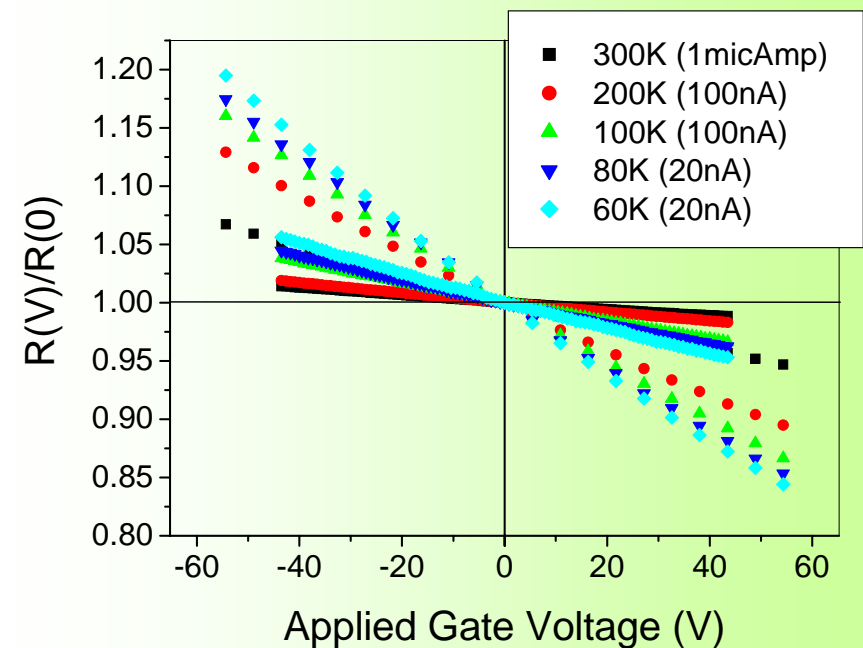
Successive Modification of the channel by the AFM tip



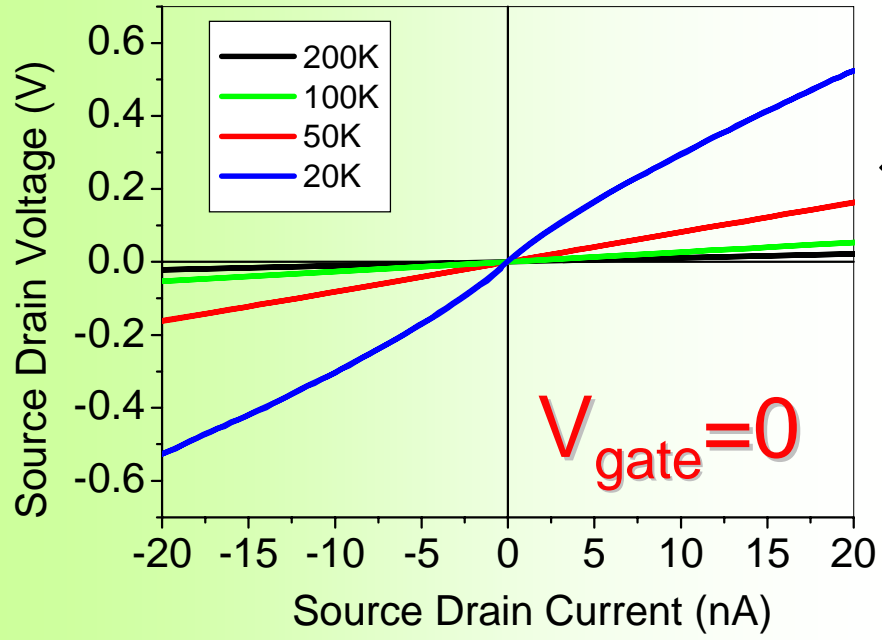
Temperature characterization of the side FET



Resistance (MOhm)

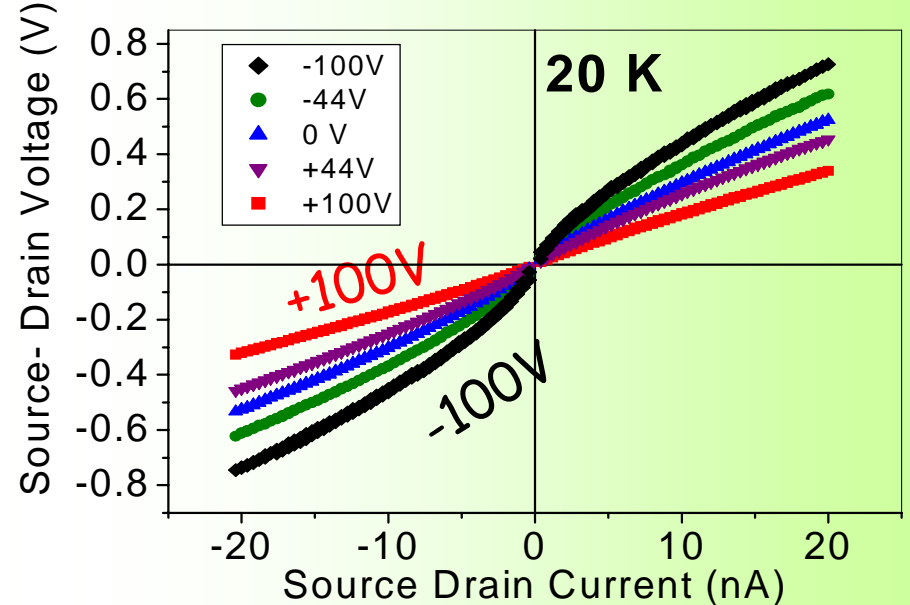
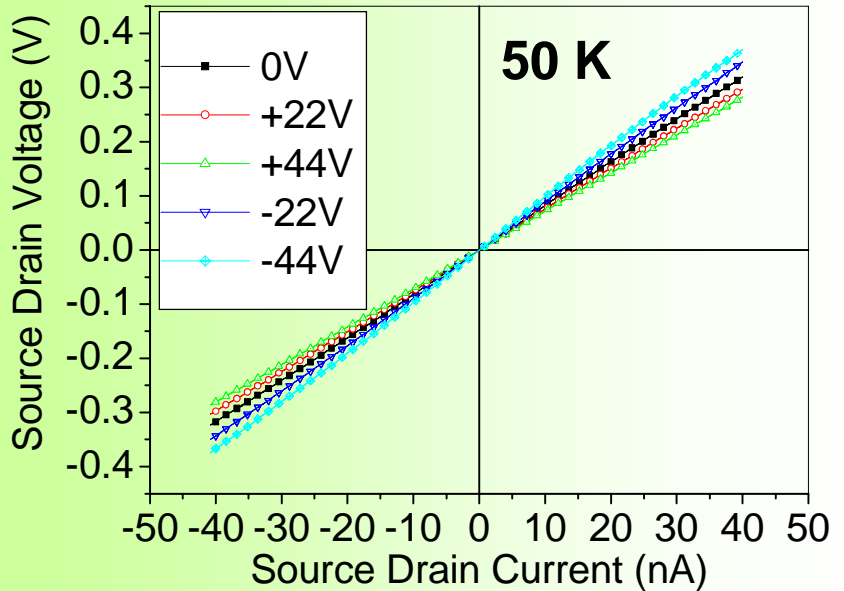


Nonlinearities in the I vs V channel behavior



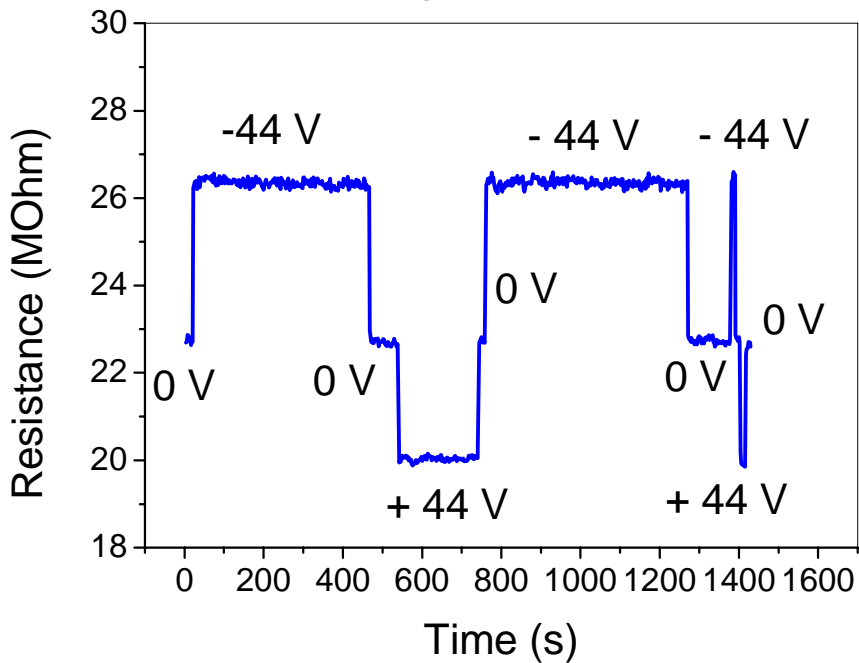
Linear to Nonlinear transition of the SD characteristics at low T

Gate modulation of the SD linearity

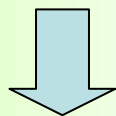


Observation of E-Field Induced Drift

20 Kelvin

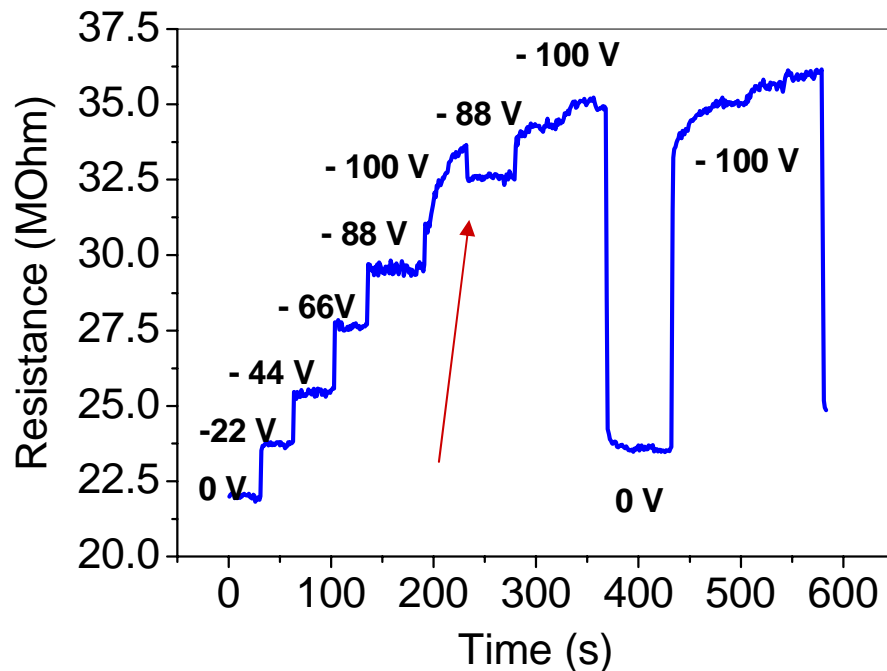


Low Gate field

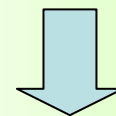


No hysteresis

20 Kelvin



High Gate field



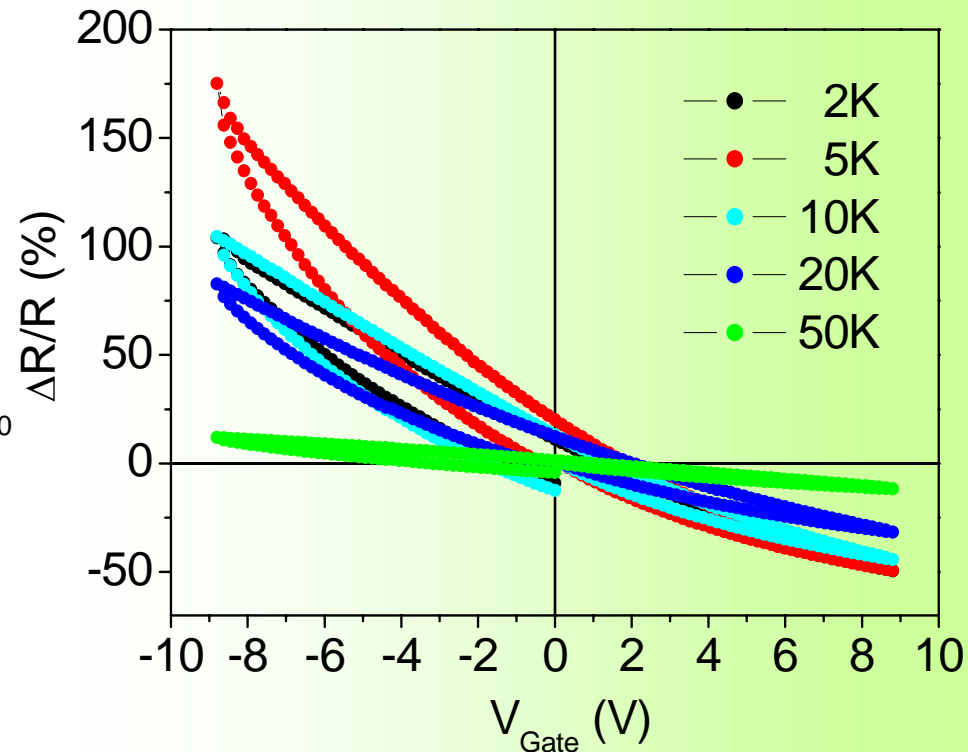
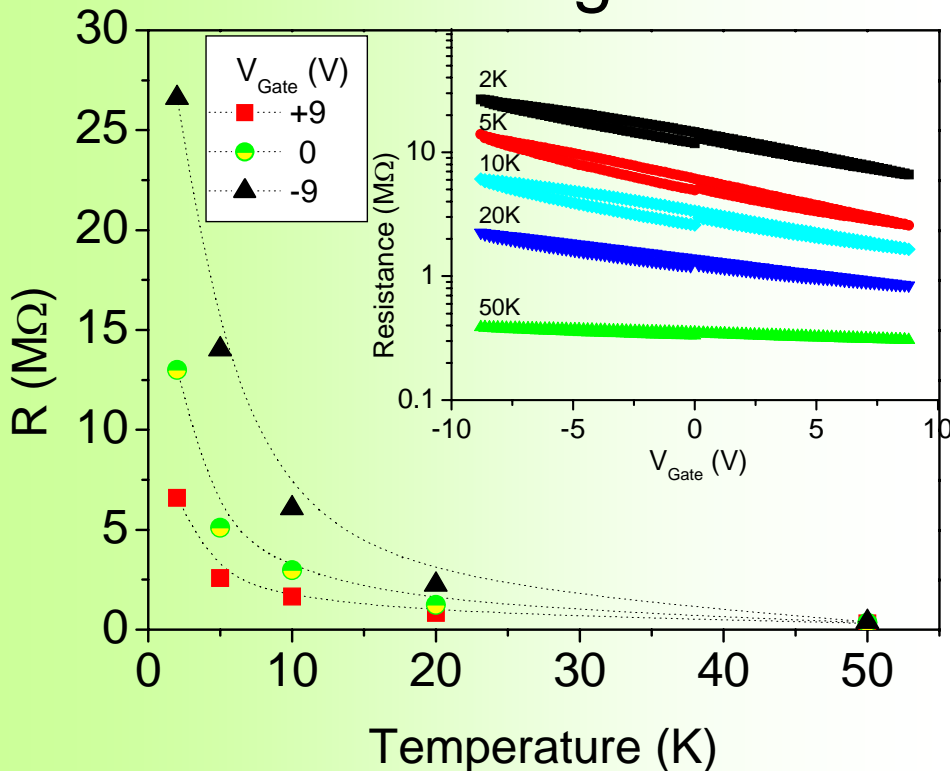
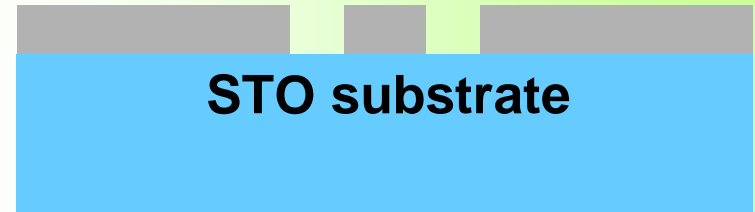
Memory effects

...Exploiting the Dielectric Constant of the Substrate

Maximum resistance modulation observed on homoepitaxial STO devices

- Homoepitaxial thin films have better conductivity
- Higher effect at lower gate voltages

STO:La on STO

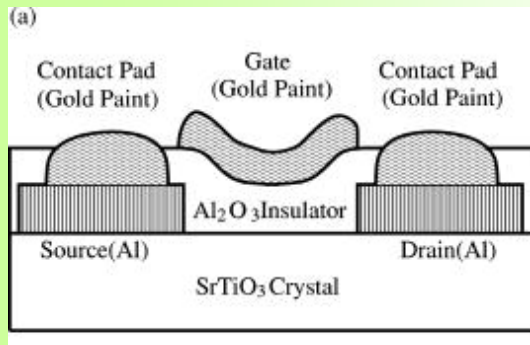


Field-effect transistor on SrTiO₃ with sputtered Al₂O₃ gate insulator

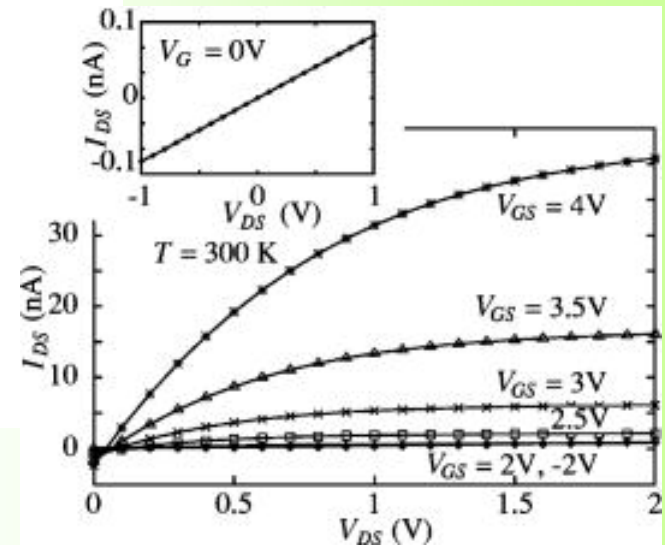
K. Ueno,^{a)} I. H. Inoue, H. Akoh, M. Kawasaki,^{b)} Y. Tokura,^{c)} and H. Takagi^{d)}
Correlated Electron Research Center (CERC), National Institute of Advanced Industrial Science and Technology (AIST), Tsukuba 305-8562, Japan

(Received 14 March 2003; accepted 1 July 2003)

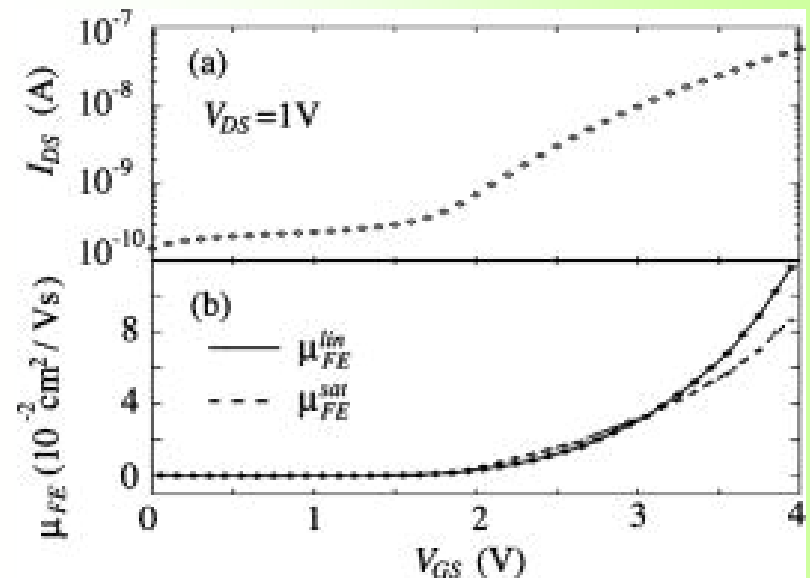
A field-effect transistor has been constructed that employs a perovskite-type SrTiO₃ single crystal as the semiconducting channel. This device functions as an *n*-type accumulation-mode device. The device was fabricated at room temperature by sputter-deposition of amorphous Al₂O₃ films as a gate insulator on the SrTiO₃ substrate. The field-effect (FE) mobility is 0.1 cm²/V s and on-off ratio exceeds 100 at room temperature. The temperature dependence of the FE mobility down to 2 K shows a thermal-activation-type behavior with an activation energy of 0.6 eV. © 2003 American Institute of Physics. [DOI: 10.1063/1.1605806]



(a) The gate-source bias V_{GS} dependence of the drain-source current I_{DS} for a fixed drain-source bias $V_{DS} = +1$ V of the same device used for Fig. 2. The on-off ratio between V_{GS} of 0 and 4 V for V_{DS} of 1 V exceeds 100. (b) V_{GS} dependence of the field effect mobility μ_{FE} . μ_{FE}^{lin} and μ_{FE}^{int} were deduced from Fig. 3(a) by using Eqs. (1) and (2), respectively. Both increase monotonically with V_{GS} and no saturation was observed even for large gate bias



Drain-source current I_{DS} plotted against the drain-source bias V_{DS} of the Al₂O₃/SrTiO₃ FET at 300 K. A channel length and a width of the FET device were 25 and 300 μ m, respectively. The inset shows the blow-up of the I_{DS} - V_{DS} curve for $V_{GS} = 0$ V



Field-effect transistor based on KTaO_3 perovskite

K. Ueno,^{a)} I. H. Inoue, T. Yamada, H. Akoh, Y. Tokura,^{b)} and H. Takagi^{c)}

Correlated Electron Research Center (CERC), National Institute of Advanced Industrial Science and Technology (AIST), Tsukuba 305-8562, Japan

(Received 16 December 2003; accepted 23 February 2004; published online 29 April 2004)

An *n*-channel accumulation-type field-effect transistor (FET) has been fabricated utilizing a KTaO_3 single crystal as an active element and a sputtered amorphous Al_2O_3 film as a gate insulator. The device demonstrated an ON/OFF ratio of 10^4 and a field-effect mobility of $0.4 \text{ cm}^2/\text{Vs}$ at room temperature, both of which are much better than those of the SrTiO_3 FETs reported previously. The field-effect mobility was almost temperature independent down to 200 K. Our results indicate that the $\text{Al}_2\text{O}_3/\text{KTaO}_3$ interface is worthy of further investigations as an alternative system of future oxide electronics. © 2004 American Institute of Physics. [DOI: 10.1063/1.1703841]

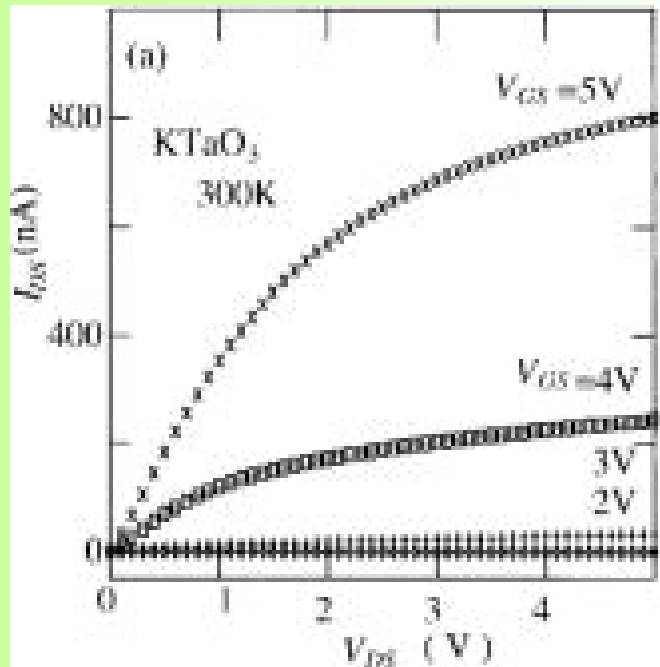


Fig. 1. (a) Drain-source current I_{DS} plotted against the drain-source bias V_{DS} of the $\text{Al}_2\text{O}_3/\text{KTaO}_3$ FET for various gate voltages V_{GS} at 300 K. The KTaO_3 single crystal was annealed at 700°C prior to the device fabrication.

Manganites

Ferroelectric-field-induced tuning of magnetism in the colossal magnetoresistive oxide $\text{La}_{1-x}\text{Sr}_x\text{MnO}_3$

X. Hong, A. Posadas, A. Lin, and C. H. Ahn

Department of Applied Physics, Yale University, New Haven, Connecticut 06520-8284, USA

(Received 28 July 2003; published 8 October 2003)

A ferroelectric field effect approach is presented for modulating magnetism in the colossal magnetoresistive oxide $\text{La}_{1-x}\text{Sr}_x\text{MnO}_3$ (LSMO). The ferromagnetic Curie temperature of ultrathin LSMO films was shifted by 35 K reversibly using the polarization field of the ferroelectric oxide $\text{Pb}(\text{Zr}_x\text{Ti}_{1-x})\text{O}_3$ in a field effect structure. This shift was also observed in magnetoresistance measurements, with the maximum magnetoresistance ratio at 6 T increasing from 64% to 77%. This model system approach does not introduce substitutional disorder or structural distortion, demonstrating that regulating the carrier concentration alone changes the magnetic phase transition temperature and leads to colossal effects.

DOI: 10.1103/PhysRevB.68.134415

PACS number(s): 73.50.-h, 75.47.Gk

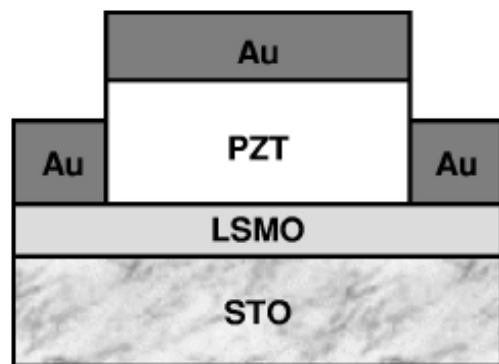


FIG. 2. Schematic view of a PZT/LSMO heterostructure deposited on a SrTiO_3 (STO) substrate. Gold electrodes are deposited for electrical transport measurements.

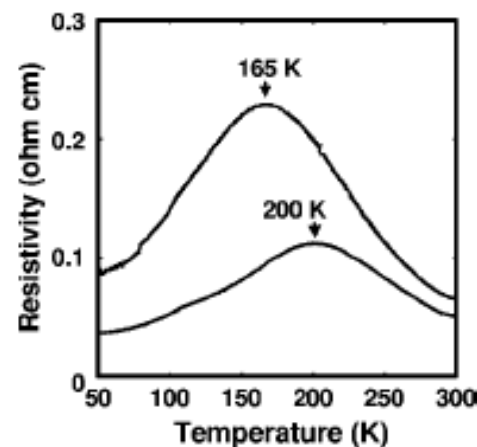


FIG. 6. Resistivity as a function of temperature for the two polarization states of the PZT layer. The upper curve corresponds to depletion of holes and is termed the depletion state; the lower curve corresponds to accumulation of holes and is termed the accumulation state. The resistivity peak temperatures are 165 K and 200 K for the depletion and accumulation states, respectively.

Side-gate devices in a $\text{La}_{0.67}\text{Ba}_{0.33}\text{MnO}_3$ exhibiting metallic behavior

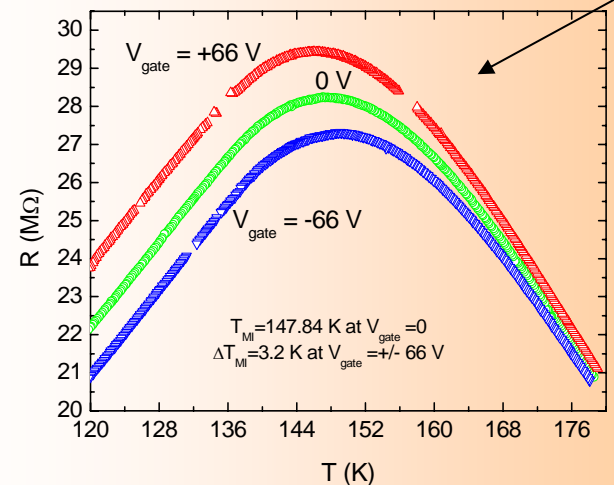
Reversible shift of the transition temperature of manganites in planar field-effect devices

patterned by atomic force microscope I. Pallecchi et al., Appl. Phys. Lett. 83, 4435 (2003)

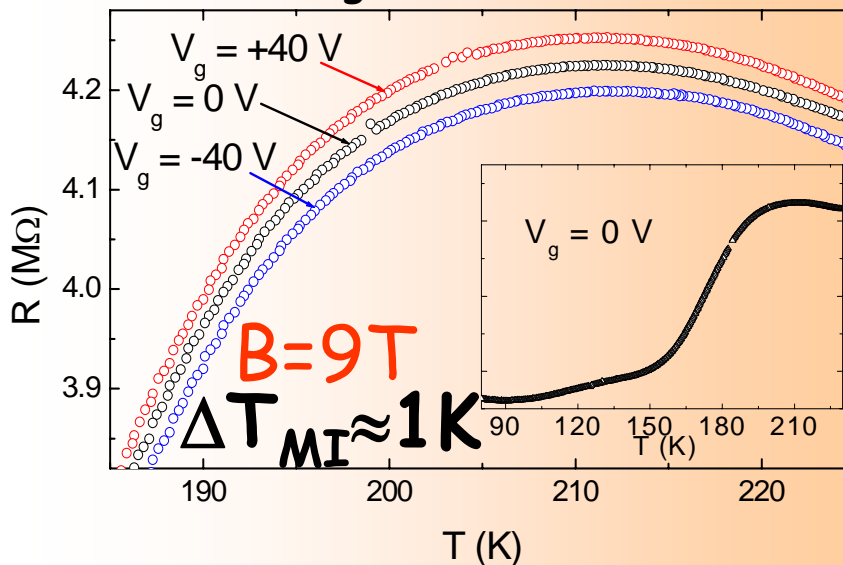
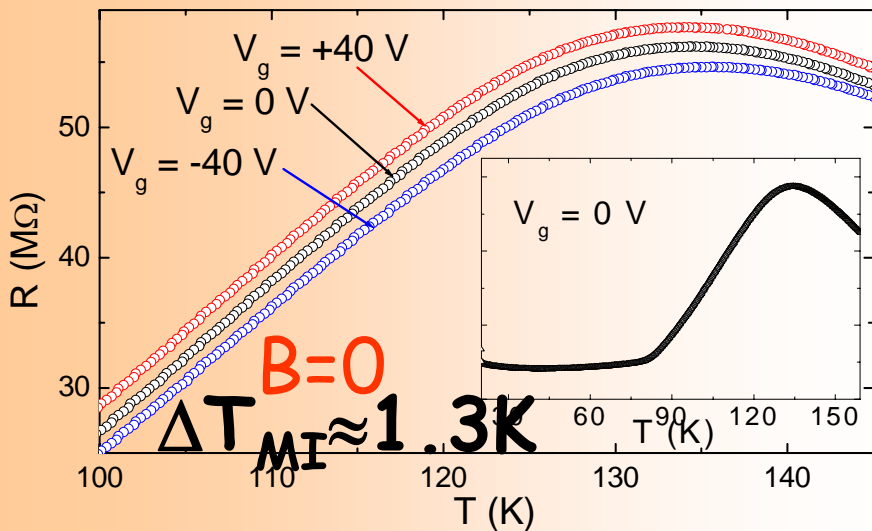
Field effect on planar devices made of epitaxial manganite perovskites I. Pallecchi et al., J. Appl. Phys. 95, 8079 (2004)

Reversible shift of the metal-semiconductor transition temperature by 3.2K

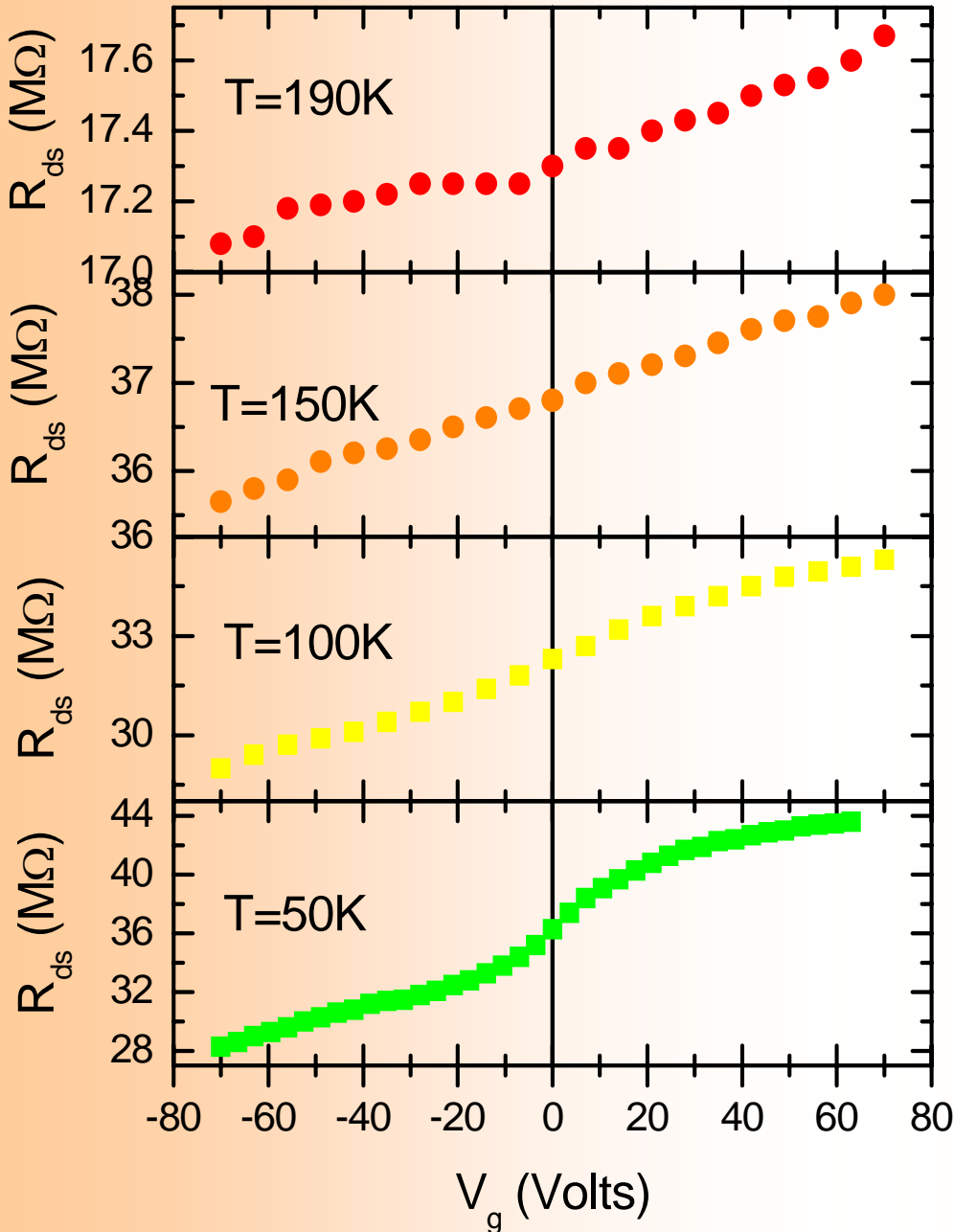
Channel width 2.3 mm
 Gate barrier width 1.4 mm
 Film thickness 22 nm $\Rightarrow C \approx 7.6 \cdot \epsilon_r$ pF/m
 For $\epsilon_r \approx 1000$, the equivalent charge per unit volume accumulated/depleted by a gate voltage of $\pm 66\text{V}$ in the channel is $6.2 \cdot 10^{19} \text{ cm}^{-3}$



Comparison of the effects of electric and magnetic fields



Is this true field effect?

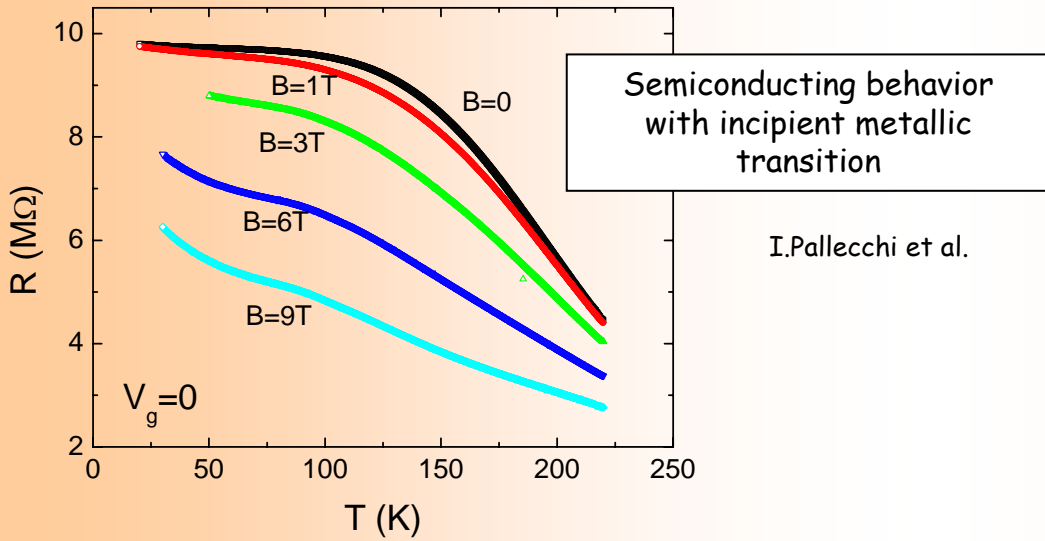


The relative change in channel resistance behavior as a function of the applied electric field is **odd** and **linear** at $T > 100K$; at lower temperature the observed non-linearities may be due to non-linear dielectric permittivity of the $SrTiO_3$ substrate.

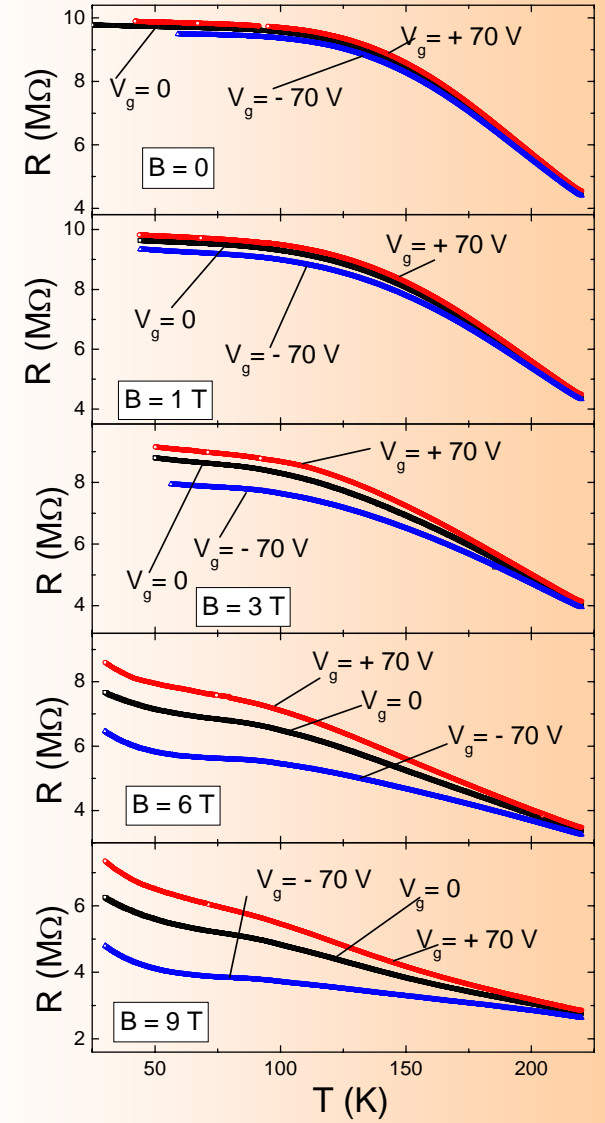
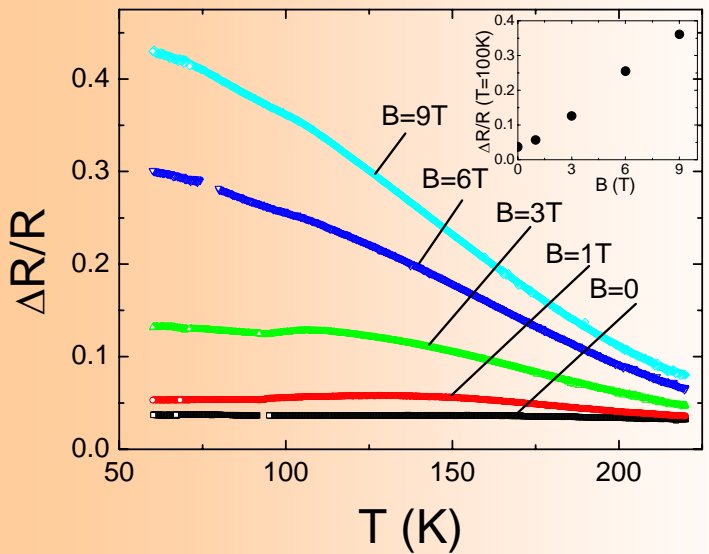
Sheet charge or volume charge?

How much in depth does the electric field penetrate in a film with more than 10^{20} carriers/ cm^3 ? Shall we invoke a **phase separation** scenario?

Side-gate devices in a $\text{La}_{0.7}\text{Sr}_{0.3}\text{MnO}_3$ below the percolation threshold



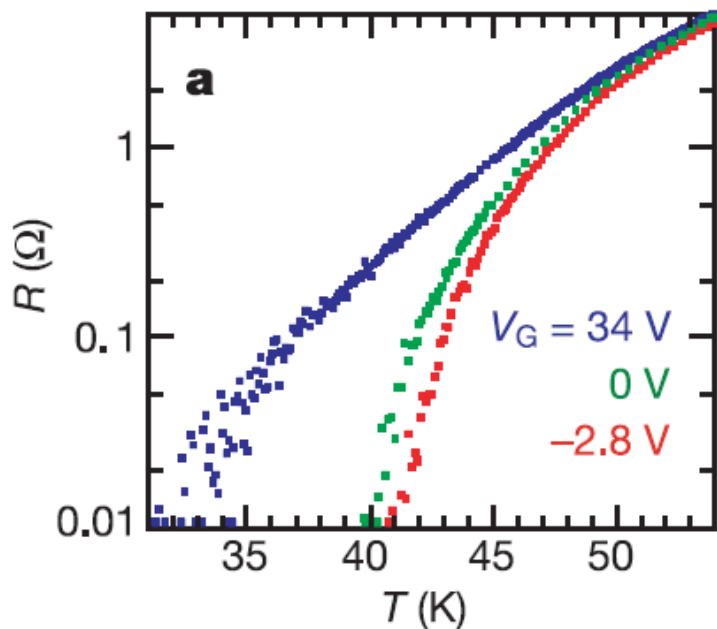
In a **phase-separation** scenario, metallic ferromagnetic regions are embedded in a semiconducting paramagnetic matrix and their volume fraction is below the percolation threshold



The electric field enlarges or shrinks the metallic ferromagnetic domains, while the magnetic field enlarges and also polarizes them.

High Temperature Superconductors

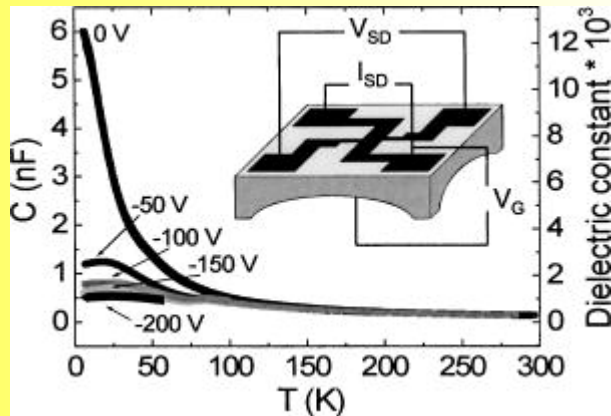
Mannhart, J. High- T_c transistors. *Supercond. Sci. Technol.* **9**, 49–67 (1996).



Field effects in superconducting films. Change of the DS resistance of an ,8-nm-thick $\text{YBa}_2\text{Cu}_3\text{O}_{7-d}$ channel with a ,300-nm-thick $\text{Ba}_{0.15}\text{Sr}_{0.85}\text{TiO}_3$ gate insulator. The blue curve corresponds to depletion of the carrier density, and the red curve corresponds to enhancement of the carrier density in the DS (drain-source) channel.

Field-effect experiments in $\text{NdBa}_2\text{Cu}_3\text{O}_{7-\delta}$ ultrathin films using a SrTiO_3 single-crystal gate insulator

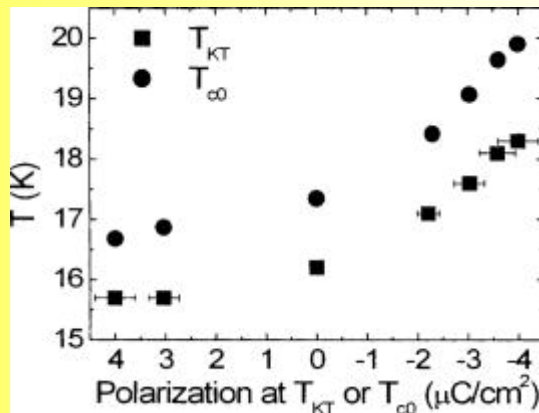
D. Matthey,^{a)} S. Gariglio, and J.-M. Triscone
DPMC, University of Geneva, 24 Quai Ernest Ansermet, 1211 Geneva 4, Switzerland



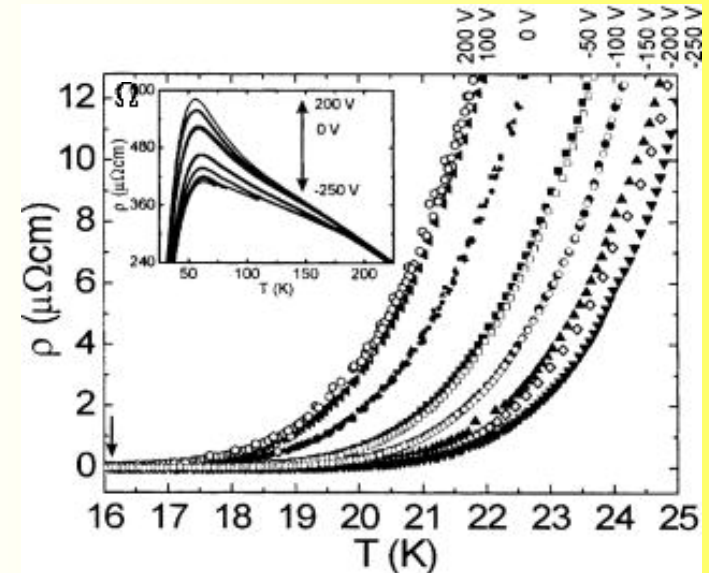
We report on the electrostatic modulation of superconductivity in very thin films of cuprate superconductors using a field-effect device based on a SrTiO_3 single-crystal gate insulator. A T_c modulation of 3.5 K and a 37% change of the normal state resistance have been observed in an epitaxial bilayer composed of an insulating $\text{PrBa}_2\text{Cu}_3\text{O}_{7-\delta}$ layer deposited on top of a superconducting $\text{NdBa}_2\text{Cu}_3\text{O}_{7-\delta}$ film, two unit cells thick. To achieve large electric fields, the thickness of the commercial dielectric single-crystal SrTiO_3 substrate (also used as the gate insulator) was reduced to $110 \mu\text{m}$. The dielectric properties of the gate insulator were characterized as a function of temperature and electric field and the magnitude of the field effect was quantified. A T_c enhancement of 2.8 K was obtained for an applied field of $-1.8 \times 10^6 \text{ V/m}$, corresponding to a polarization of $-4 \mu\text{C/cm}^2$. © 2003 American Institute of Physics. [DOI: 10.1063/1.1624635]

Temperature and electric field dependence of the capacitance and dielectric constant of the STO single-crystal gate insulator. Inset: schematic of the device

Resistivity as a function of temperature of the PBCO/NBCO heterostructure close to the foot of the transition and over the whole temperature range (inset) for different applied fields across the gate dielectric. The resistivity was calculated using the thickness of the NBCO layer. The arrow indicates the value of TKT for zero applied field.



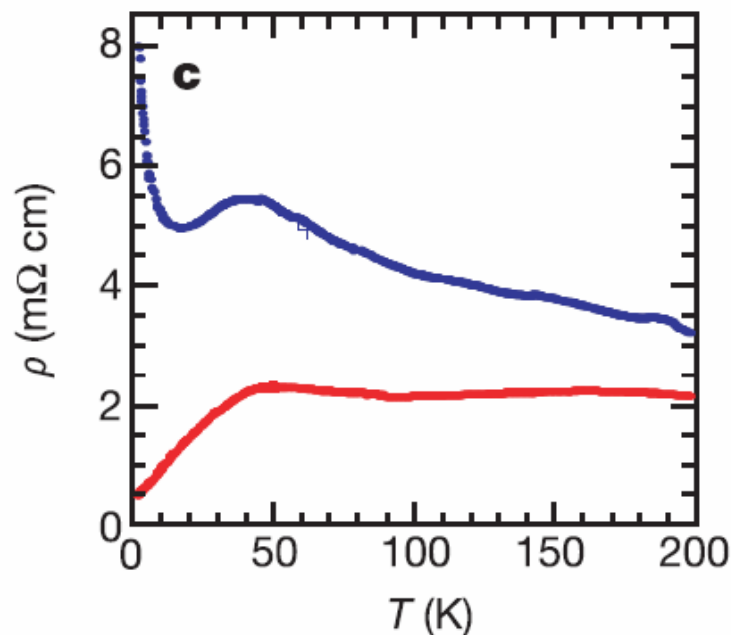
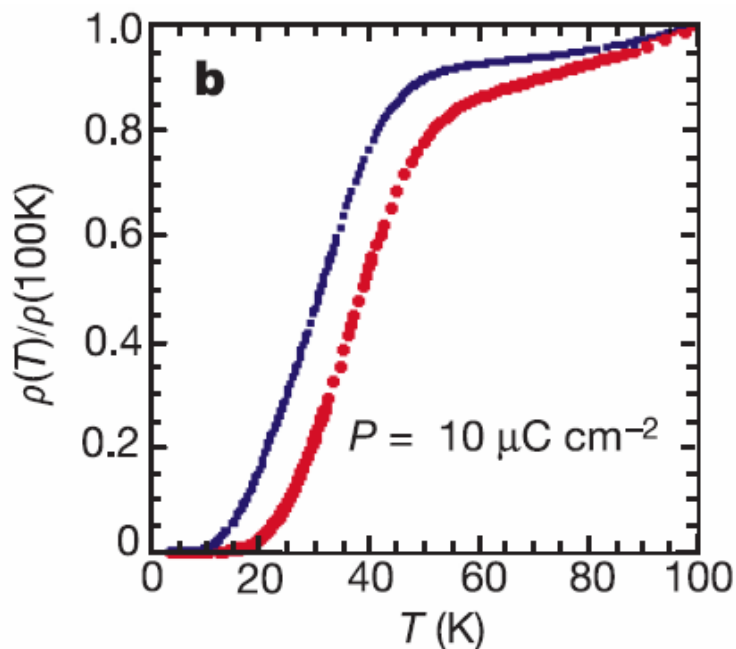
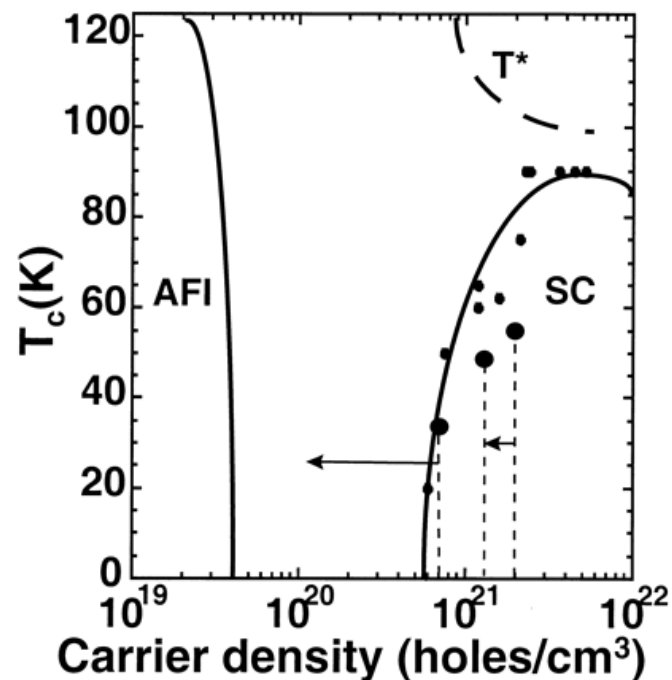
Critical temperature T_{KT} (the Kosterlitz–Thouless temperature), and T_{c0} , the temperature at which $R=0.1$ of the NBCO layer as a function of the measured polarization at T_{KT} or T_{c0}



Electrostatic Modulation of Superconductivity in Ultrathin $\text{GdBa}_2\text{Cu}_3\text{O}_{7-x}$ Films

C. H. Ahn, S. Gariglio, P. Paruch, T. Tybell, L. Antognazza, J.-M. Triscone

The polarization field of the ferroelectric oxide lead zirconate titanate [$\text{Pb}(\text{Zr}_x\text{Ti}_{1-x})\text{O}_3$] was used to tune the critical temperature of the high-temperature superconducting cuprate gadolinium barium copper oxide ($\text{GdBa}_2\text{Cu}_3\text{O}_{7-x}$) in a reversible, nonvolatile fashion. For slightly underdoped samples, a uniform shift of several Kelvin in the critical temperature was observed, whereas for more underdoped samples, an insulating state was induced. This transition from superconducting to insulating behavior does not involve chemical or crystalline modification of the material.

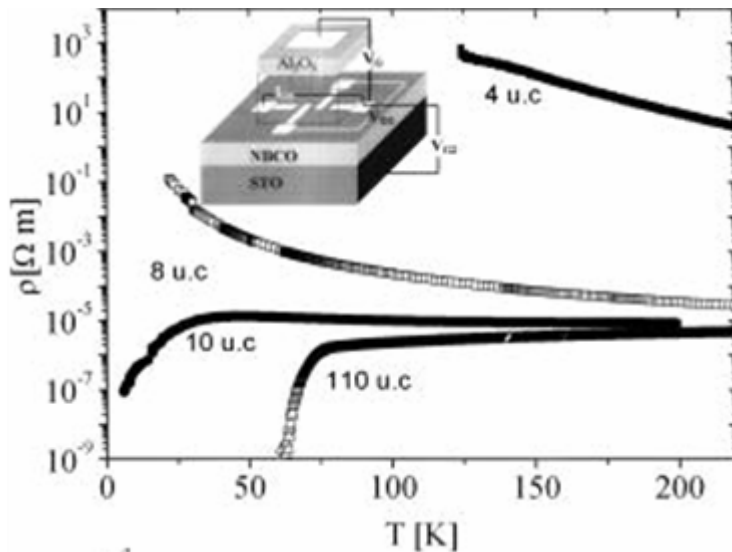


Field-effect tuning of carrier density in $\text{Nd}_{1.2}\text{Ba}_{1.8}\text{Cu}_3\text{O}_y$ thin films

A. Cassinese, G. M. De Luca, A. Prigobbo, M. Salluzzo,^{a)} and R. Vaglio
INFN-COHERENTIA, Dipartimento di Scienze Fisiche, Università di Napoli Federico II, Napoli, Italy

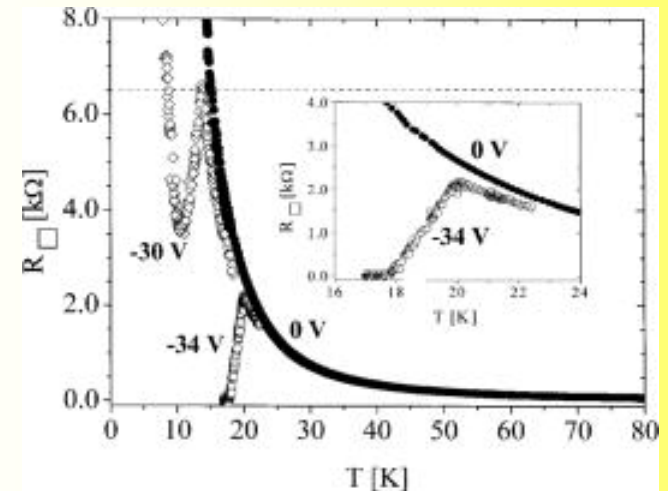
(Received 5 January 2004; accepted 14 March 2004; published online 29 April 2004)

Using a field effect device we modified the number of holes in the surface layers of 4 to 10 unit cell $\text{Nd}_{1.2}\text{Ba}_{1.8}\text{Cu}_3\text{O}_y$ (NBCO) epitaxial films grown on (100) SrTiO_3 substrates. The results obtained on a set of 12 devices demonstrate that it is possible to induce reversible changes of the hole density of NBCO films by field effect. It is found that the field effect becomes less pronounced increasing the film thickness. Insulating–superconducting transition was observed in one 8 unit cell NBCO field effect device. © 2004 American Institute of Physics. [DOI: 10.1063/1.1745103]



Sheet resistance measured as a function of temperature on an 8 u.c. FET for $V_g = 0$ (closed circles), $V_g = -30$ V (open diamonds), and $V_g = -34$ V (open circles). The dashed line indicates the value of the quantum resistance $R_Q = 6.45$ k Ω . In the inset the insulating–superconducting transition is shown

Temperature dependence of the resistivity of $\text{Nd}_{1.2}\text{Ba}_{1.8}\text{Cu}_3\text{O}_y$ films having different thicknesses: 4 u.c. (closed squares), 8 u.c. (open squares), 10 u.c. (closed circles), and 110 cells (open triangles). In the inset a sketch of the field effect device is shown.



Conclusions

- Field effect in transition metal oxides is possible adopting new geometries and high- κ materials.
- Back and side gate geometry allow direct access to the channel under FE
- In ZnO the application is close
- FE proved to be a powerful tools for the study of strongly correlated electron system:
 - Magnetic transition and phase separation in manganites
 - Superconducting properties in HTCS